The Effect of Variabilities in the Manufacturing Tolerances on the Ultimate Flexural Capacity of Steel Beams

Abigail Debono

Dissertation submitted to the

Faculty for the Built Environment

University of Malta

In part fulfilment of the requirements for the attainment of the degree

Master of Engineering

(Structural Engineering)

July 2024

L-Università ta' Malta

University of Malta Library – Electronic Thesis & Dissertations (ETD) Repository

The copyright of this thesis/dissertation belongs to the author. The author's rights in respect of this work are as defined by the Copyright Act (Chapter 415) of the Laws of Malta or as modified by any successive legislation.

Users may access this full-text thesis/dissertation and can make use of the information contained in accordance with the Copyright Act provided that the author must be properly acknowledged. Further distribution or reproduction in any format is prohibited without the prior permission of the copyright holder.

L-Università ta' Malta

FACULTY/INSTITUTE/CENTRE/SCHOOL for the Built Environment

DECLARATIONS BY POSTGRADUATE STUDENTS

(a) Authenticity of Dissertation

I hereby declare that I am the legitimate author of this Dissertation and that it is my original work.

No portion of this work has been submitted in support of an application for another degree or qualification of this or any other university or institution of higher education.

I hold the University of Malta harmless against any third party claims with regard to copyright violation, breach of confidentiality, defamation and any other third party right infringement.

(b) Research Code of Practice and Ethics Review Procedures

I declare that I have abided by the University's Research Ethics Review Procedures. Research Ethics & Data Protection form code BEN-2024-00008.

As a Master's student, as per Regulation 77 of the General Regulations for University Postgraduate Awards 2021, I accept that should my dissertation be awarded a Grade A, it will be made publicly available on the University of Malta Institutional Repository.

To My Family

Acknowledgments

First and foremost, I would like to sincerely offer my gratitude to my mentor, Dr. Jeanette Abela Munoz, B.E.&A.(Hons)(Melit.),M.Sc.(Lond.),Ph.D.(Lond.), who has supported me throughout my years at university, guiding me with patience and engaging discussions throughout this dissertation and beyond.

I would like to express my deepest gratitude to my family: my parents, Franco and Daphne, my brother, Daniel, and my dogs, Hope and Mike. Their constant presence, unwavering love, and support have been my foundation not just during this dissertation but throughout the entire course. I also want to extend my gratitude to my friends, most especially Luke and Kurt, for their thoughtful discussions and constant encouragement. Without them, this dissertation would not have been possible.

I take full responsibility for any shortcomings in this dissertation.

Abstract

Steel fabrication involves the production of large, complex welded assemblies of rolled steel products, inherently leading to dimensional variations due to high-temperature processes used in manufacturing and joining. The purpose of this research is to examine the validity and safety of the tolerance tables established by the Eurocode (EN10034: 1993) in terms of the ultimate flexural capacity of the beam. Both geometric properties and material properties have been treated as random variables. With the Monte Carlo Simulation, 2000 realistic and randomised combinations were produced in order to compare the randomised moment capacity with the nominal plastic moment capacity.

The analysis began with a comprehensive test in which all variables were randomised. This initial test provided the probability of failure for all beams under realistic conditions. Subsequent tests were conducted with certain variables held constant at their nominal values to assess the influence of each random variable on the plastic moment capacity. Further detailed analysis involved three purposely selected beams—specifically IPE80, IPE360, and IPE750x173—chosen for their varied section depths. The results from these tests were depicted in scatterplots, which facilitated the visual identification and understanding of any trends previously noted in the general analysis.

Through the in-depth analysis, it was concluded that the flange thickness is the most critical dimensional property across all section sizes. Additionally, a highly important controlling factor is the variability of the yield stress. In fact, the in-depth analysis demonstrated that the effect of the remaining three-dimensional variables on the plastic moment capacity varies by section size. Specifically, the geometric properties, such as section height and width of section, have a diminishing influence as the section size increases, while the impact of web thickness on the probability of failure becomes more pronounced with larger section sizes.

Keywords: Tolerances, Geometric Properties, Material Properties, Monte Carlo Simulation, Flexural Capacity

Table of Contents

List of Figures

List of Tables

Notation

A	Cross-sectional Area
A_v	Shear Area
E	Young's Modulus
EI	Flexural Rigidity
F_R	Distribution Function of Strength
F_S	Distribution Function Load Effect
F_u	Ultimate Tensile Strength
F_y	Yield Strength
G	Shear Modulus
h_s	Section Height
I	Moment of Inertia
J	Torsional Constant
M	Bending Moment
M	Safety Margin
M_o	Yield moment
M_p	Plastic Moment
P_f	Probability of Failure
R	Resistance Variables
R	Radius of curvature
R	Radius of gyration
S	Loading Variables
S_o	Yield Stress for Steel
$S_{o.charc}$	*Characteristic Yield Stress*
$S_{o.\ Mean}$	*Mean*
$S_{o.COV}$	*Coefficient of Variation*
$S_{o.stand.dev}$	*Standard Deviation*
t_w	Web Thickness
t_f	Flange Thickness
w_s	Width of Section
z	Plastic Section Modulus
β	Reliability Index

μ_M	True Value of M
μ_R	True Value of R
μ_S	True Value of S
σ_M	Standard Deviation of M
σ_R	Standard Deviation of R
σ_S	Standard Deviation of S
σ	Stress
ε	Strain
τ	Shear Strain
γ	Shear Stress
ε_l	Axial Strain
ε_t	Transverse Strain
ν	Poisson's ratio
$\boldsymbol{\phi_y}$	Yielding curvature
γ_M	Partial Safety Factor for Material
γ_f	Partial Safety Factor for Material

1 Introduction

In the construction industry, steel is a cornerstone that is a well-recognized for its essential function in structural systems. Steel beams, in particular are essential since they are extensively used and not only to withstand loads but also enhance the resilience of the structure. Even though steel beams are widely used and have many applications, the manufacturing process adds intrinsic complexity, most notably tolerances.

The allowable limit of variation in a dimension can be described as a tolerance. In manufacturing processes, the tolerance recognizes the highest and minimum limits that a beam can withstand while maintaining optimal functionality. The Eurocode allows for slight variation that can occur naturally during the manufacturing process, and in fact, it defines the geometric dimensional tolerances for steel beams.

This dissertation explores the suitability of the tolerances for steel beams as defined by the Euronorm, EN10034:1993, critically analysing them through Monte Carlo Simulations to investigate their applicability in practical contexts. This study attempts to provide insights into how the dimensional tolerances influence the reliability of steel beams' ultimate flexural capacity.

1.1 Research Questions

- To what degree are the geometrical tolerances established by the Euronorm , EN 10034, safe in terms of plastic moment capacity?
- To what degree do each geometrical tolerances influence the probability of failure?
- Which dimensional variation is the most critical, and how should variations be managed to ensure that the nominal plastic moment capacity is still achieved?

1.2 Aims

- Conducting a thorough analysis on the specified ranges and their intended safety margins.
- Carrying out a Monte Carlo simulation to produce a variety of random generations each of which reflects a unique set of Eurocode tolerances.
- Creating a calculator able to determine the plastic moment capacity for each randomly generated beam (as stated in the previous point) and comparing it with the nominal plastic moment capacity in order to analyse any failure probabilities.
- Establishing a statistical analytical system results to determine which variable is most critical on the overall structural capacity of the beam.

1.3 Objectives

- To evaluate the safety of the geometrical tolerances that are specified for steel I-sections by the Euronorm, EN10034 (1993).
- To generate probabilistic scenarios using the Monte Carlo simulation that depict how steel I-sections behave when they have various tolerances.
- To understand how various combinations of variable randomness and constancy affect the steel IPE beam's plastic moment capacity.
- To determine any observable patterns or trends in the failures, as well as important variable combinations that have a substantial impact on the probability of failure.

1.4 Dissertation Overview

This document comprises three main sections: the literature review, the methodology, and the results.

Chapter 1: Introduction

In this chapter, the dissertation provides an overview of the research topic and it presents the motivation behind the study, introducing the problem statement related to the tolerances table and the probability of failure concerning the plastic moment capacity. It highlights the significance of the research and provides a brief outline of the subsequent chapters.

Chapters 2 & Chapter 3: Literature Review

Chapter 2 explores the significance of steel beams, focusing on their material properties and their vital role in construction. This chapter also delves into the critical aspects of elastic and plastic bending in structural applications.

Chapter 3 is a continuation of the literature review that presents the importance of standardizing such a used construction component in the engineering world. This chapter also discusses the importance of the Eurocode and how the code itself sets limits to the tolerance of the steel beam. The limit state principle is analysed in detail, as this will be applied within the methodology.

Chapter 4: Methodology

This chapter presents the setup of the Monte Carlo Simulation, a widely accepted and reliable method in the field. It also details the importance of how each geometrical variable is considered a variable within the runs, ensuring a comprehensive and accurate analysis. This chapter also explains the different tests that are carried out. Furthermore, this section discusses the limit state principle and how it plays an important role within the methodology.

Chapter 5 Discussion of Results

This chapter presents and discusses the results. It explores all the results from all three tests and the effects of different combinations of variables and how they influence the probability of failure. The findings give a practitioner an idea of which geometrical variable/s should be checked when designing plastically.

Chapter 6 Conclusion and Recommendations for Future Work

All the key findings that have been drawn from this study will be presented within this chapter. It will reflect back on what aims and objectives were presented in chapter 1 and whether they have been achieved satisfactory. Based on the research findings , this chapter offers recommendations for future research and areas that require further investigation.

2 Literature Review

2.1 Introduction

The use of structural steel dates back to 1858 when Henry Bessemer developed a process to convert molten pig iron into steel. In the late 19th century, mild steel replaced wrought iron and cast iron. In fact, in 1889, the first major structure made of steel was constructed. This landmark is known as The Forth Bridge. Nowadays, steel remains a popular choice within the construction industry due to its diverse properties, including strength, durability, malleability, and ease of fabrication. In fact, steel is commonly used for structural elements and concrete-steel reinforcement. From a structural engineer's perspective, the steel's material and geometric properties dictate the strength characteristics of any steel element. (Moynihan & Allwood, 2024)

Steel is produced through various processes, initiated by the melting of iron ore in a blast furnace, followed by the refinement of the molten iron, and finally the adjustment of the composition through alloying. Current steel production techniques include the Basic Oxygen Furnace (BOF) and the Electric Arc Furnace (EAF). However, due to the variability in material and geometric properties between nominally identical samples, Eurocode, EN1993-1-1 (2005) provides partial safety factors which are incorporated in the structural engineering practice to reduce the safety load resistance of the structural element.

2.2 Material Properties

The amount of carbon content mixed with iron determines the grade and type of alloys, such as mild steel and cast iron. Carbon is an important alloying element in steel, but iron is the primary constituent. In plain carbon steel, the properties are primarily influenced by carbon content (as shown in figure 2.1) with additional amounts of other elements, typically less than 0.5% silicon and 1.5% manganese. An increase in carbon content leads to increased hardness and strength due to the formation of the hard and brittle cementite. However, this increase in carbon content also results in decreased ductility and toughness (Epri & Gandy, 2006).

The above description renders steel as a versatile material whose properties can be modified to the desired application by carefully selecting the quantities of the raw materials and manufacturing techniques. Engineers can select the material's properties based on the use of the structural component requirement. The mechanical properties of steel are of utmost importance, particularly in

most engineering applications. Yield strength, ultimate tensile strength, elastic modulus, and shear modulus are the critical parameters that define a material's performance.

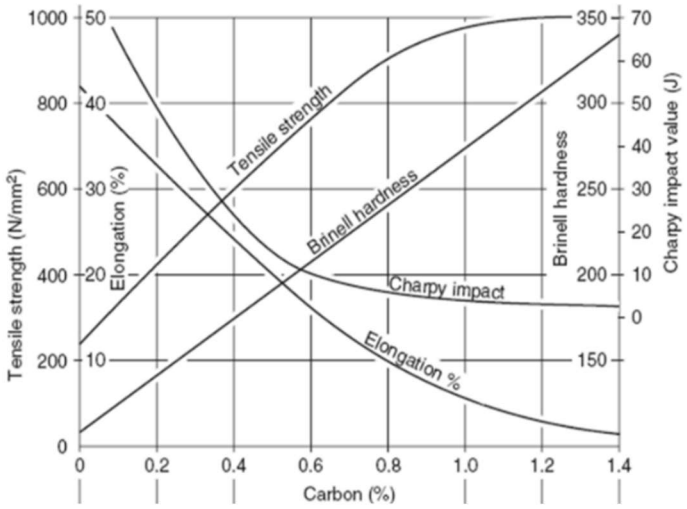

Figure 2.1 | Effect of carbon content on mechanical properties of steel (Epri, D. & Gandy 2006)

2.2.1 Yield Strength

Yield strength (f_y) is an indispensable parameter that plays a vital role in the engineering world, particularly in the design of structures. It defines the maximum stress a ductile material can resist before utilising the plastic capacity of the same material. This mechanical property is essential for engineers to understand the behaviour of materials under stress, which helps them select the most suitable grade for various applications.

Knowing the yield strength of a material is important for ensuring the structural stability of buildings, bridges, and other crucial infrastructure. In engineering, selecting materials and defining the geometrical properties to withstand the stresses that can be encountered in the real world is fundamental. An analysis of a material's stress-strain graph can determine its yield strength[1] (Figure 2.2).

Strain (ε) is defined as the ratio of a dimension's length change (extension) to the dimension's original length, while stress (σ) refers to the ratio of applied force to cross-sectional area. Therefore, by analysing the slope of the stress-strain graph, which occurs only within the elastic region of the material, engineers can determine the yield strength of a material. Hooke's Law[2] is the theory used

[1] Stress-strain graphs are graphical representations of a material's behaviour when subjected to stress. The graph's y-axis represents the stress, whilst the x-axis represents the strain.

[2] Hooke's Law states that the displacement or size of a deformation in an object is directly proportional to the deformation force, provided the deformations are relatively small. When the load is removed, the object returns to its original shape and size under these conditions. (Williams, 1956)

during laboratory testing of a steel element when determining its respective stress-strain graph. The methodology is based on an established tensile test (refer to standard EN ISO 6892-1). (T. A. Philpot, 2019)

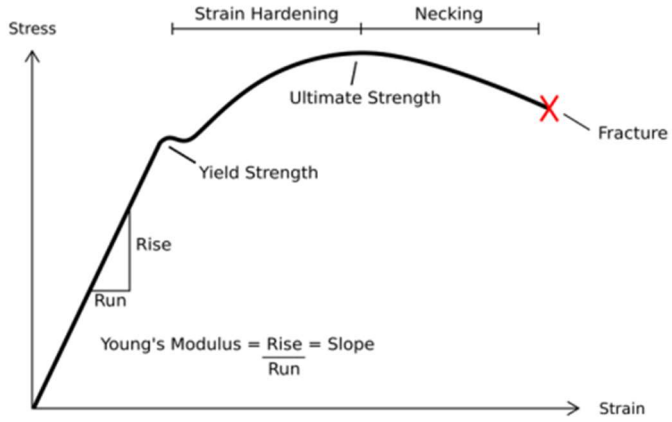

Figure 2.2 | Schematic stress-strain curve with notation (Philpot, T. A. 2019)

2.2.2 Ultimate Tensile Strength

Another crucial mechanical characteristic that dictates the highest load a material can sustain before beginning to deform plastically and ultimately failing is the Ultimate Tensile Strength (F_u). It is typically defined as the curve's highest point. In fact, it indicates that the material has already gone through the strain hardening zone before it reaches the UTS. The material stiffens and gets stronger during strain hardening as a result of crystalline structure rearrangement and dislocation movement.

Once the UTS is reached, the steel element enters the necking zone, where localised deformation causes the material to narrow drastically at one point along its length. The UTS is the point at which the material is under severe considerable stress. Furthermore, necking causes an abrupt failure point where the material is unable to withstand the strain and fails. (Philpot, T. A. 2019)

2.2.3 Elastic Modulus

Young's Modulus (E), also known as the Elastic Modulus, is another significant material property that indicates the stiffness of the material. The stiffness property of a material determines the material's ability to resist deformation when subjected to compression or tensile forces. As previously mentioned, elastic energy is stored in a material; as mentioned previously, the stress-strain graph summarises this process and shows how the material's energy is either dissipated in the form of elastic or plastic strains. (Popov, E. P. 1998)

The surface area of a material is closely correlated with its rate of deformation when it is undergoing elastic deformation. Therefore, the strain and the stress of the same material are linked by Hooke's Law (Eq.1).

$$E = \frac{\sigma}{\varepsilon} \qquad \textit{Eq.1}$$

The respective tests for tension, bending, and natural frequency can all be used to determine the modulus of elasticity of a material. These tests are referred to as static methods as they are entirely based on the Principle of Hooke's Law.

2.2.4 Shear Modulus

When transverse internal forces like torsion and twisting are applied to a material, its elastic characteristics are described by a numerical constant called the shear modulus (G), also known as the rigidity modulus. Any small cubic volume within the material is being distorted, in a way that two of its faces slide parallel to one another and the two faces transform from square to diamond. Within the elastic limit of the material, the modulus quantifies the ratio of shear stress[4] to shear strain[5] within the material's elastic limit ().

$$G = \frac{\tau}{\gamma} \qquad \textit{Eq.2}$$

2.2.5 Poisson's Ratio

Generally, when a material is stretched, it tends to contract in two directions that are opposite to each other(Fig.2.3). When a rubber band is stretched, it becomes significantly thinner, and this phenomenon is known as the Poisson effect. Contrarily, a material expands in directions that are transverse to the direction of compression when it is compressed as opposed to stretched. Poisson's ratio *(ν)* thus illustrates the percentage of strain passively supplied perpendicular to the primary strain (Eq. 3)

$$\nu = \frac{-\varepsilon_t}{\varepsilon_l} \qquad \textit{Eq.3}$$

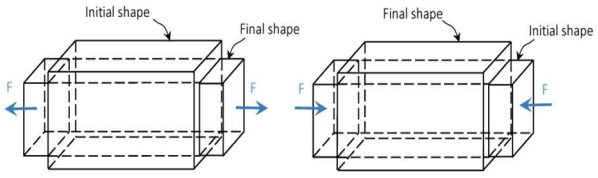

Figure 2.3 | Lateral contraction and expansion of solid bodies subjected to axial forces (Poisson effect) (Popov, E. P. 1998)

[4] Shear Stress is the measurement of the force applied parallel to the surface of a material divided by the area over which it is distributed.

[5] Shear Strain measures the degree of deformation a material experiences relative to its initial dimension, specifically the horizontal shift relative to its height.

2.3 Geometric Properties

For the purpose of this research, a number of steel IPE beams (IPE80, IPE160, IPE240, IPE360, IPE450, IPE600 AND IPE750X173) are going to be investigated. (The manufacturing process and the origin of the beam shape will be discussed in Chapter 3.) The geometric property of a beam is also a crucial factor that should be considered during the structural design and analysis of a structure. The geometric properties that define the shape of the I-beam are (as graphically presented in Figure 2.4 |) :

- The depth of section
- The width of section
- The web thickness
- The flange thickness
- The root radius (located at the web-flange junction)

These dimensions would dictate how the stress is distributed throughout the beam's material. Therefore, the geometric properties would consequently influence other factors, such as;

- Cross-Sectional Area (A)
  - The total area of the cross-section perpendicular to the beam axis.

- Moment of Inertia (I)
  - A measure of the distribution of the cross-sectional area around the axis of bending. It influences the beam's resistance to bending (in the respective direction of the beam's axis) and is a key parameter in calculating bending stress.

- Torsional Constant (J)
  - A measure of a section's resistance to twisting loads. It is applicable in analysing the torsional behaviours of beams.

- Section Modulus (S)
  - The ratio of the moment of inertia to the distance from the neutral axis to the outermost fibre of the section. It is a critical parameter in bending calculations used to determine bending stress.

- Shear Area (A_v)
  - The effective area for resisting shear forces in the cross-section. It is relevant in calculating the shear stress in the beam. A measure of how the area in the cross-section is distributed

relative to an axis. It provides an indication of how slender[6] or stocky[7] a section is with respect to bending.

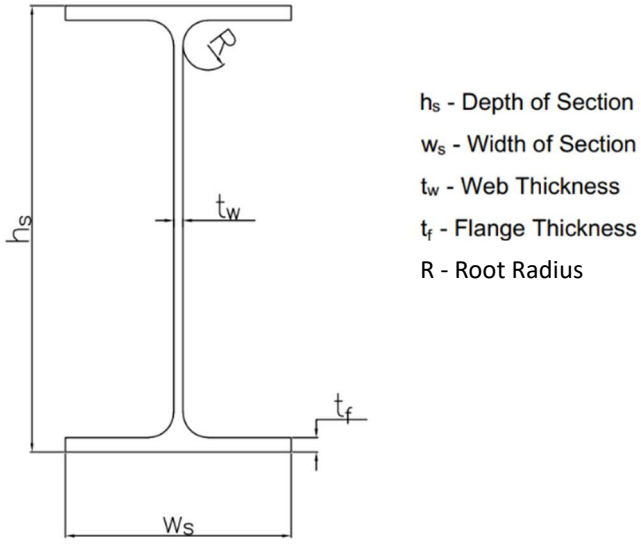

Figure 2.4 | Geometric Properties that define the shape of an IPE beam (Author, 2024)

[6] Slender Section: A structural element that is relatively long and slender in comparison to its cross-sectional dimensions.

[7] Stocky Section: A structural element that is short and more stout compared to its cross-sectional dimensions.

2.4 Introduction of Steel Beams in Bending

The study of *beam bending* originated from Galileo's study back in 1564, when he carried out a systematic analysis of a cantilever beam. His aim was to analyse the force required to reach the bar's tensile breaking (failure) point. However, it was Saint-Venant who developed the plastic bending hypothesis by carrying out further research on non-linear elastic materials[8]. In fact, multiple literature refer to Saint Venant's model as the fundamental study of beam behaviour. Moreover, the developed 3D model allowed the analytic behaviour of the beam-like solid in terms of 3D stress analysis and displacement fields. (Yu T. X. & Zhang, L.C.1996)

Steel beams subjected to a load along the length of the member are common structural components that are used in various engineering applications. The beam is only able to withstand the load by bending action, resisting the deformed deflection. Bending actions stem from a beam's flexural capacity, which is its ability to resist a load using compressive and tensile stresses. As shown in the figure below (Figure 2.5), for simply supported beams, the bottom fibres of the beam, will be subjected to tension, whilst on the top face, it will be subjected to compression.

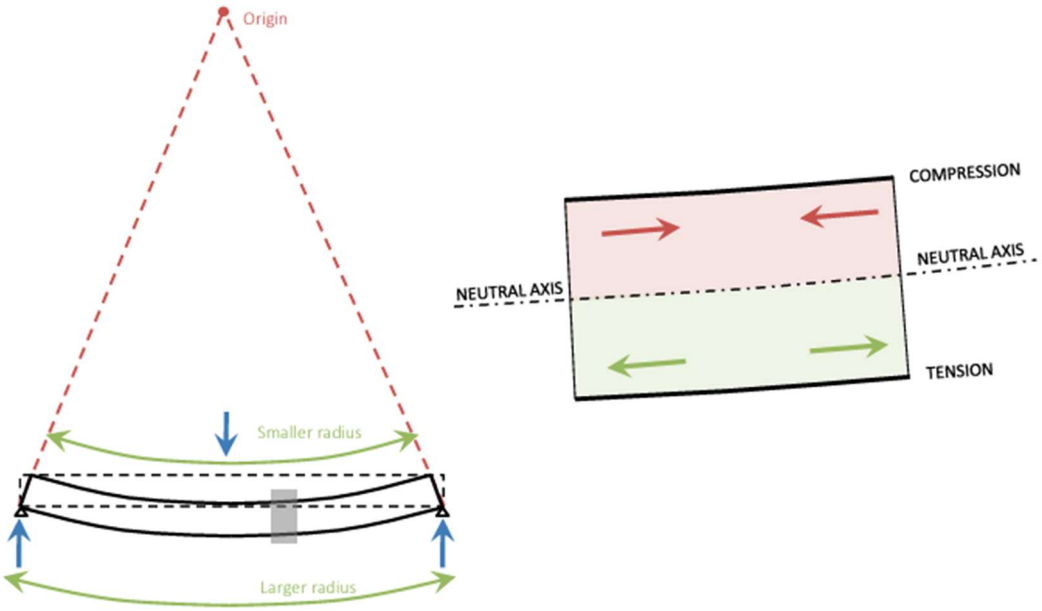

Figure 2.5 | Bending of a simply supported beam with a schematic diagram of the forces acting at cross-section (Popov, E.P. 1998)

[8] Non-Linear Elastic Materials: Materials that do not exhibit Hooke's Law.

2.4.1 Theory Of Elastic Bending Of Beams

The following section focuses on the simplest form, which is a slender element that is subjected to transverse loading and is referred to as the beam. Beams are designed on two criteria (1) limited deflection and (2) strength. There are two possible configurations for the transverse loading: *concentrated* and *distributed.* The concentrated load, also known as a point load, is a force that is applied at one point on the beam. Whilst a distributed load is a force that is applied over the entire length of the beam. Additionally, the distributed load can be of two types, uniform distributed load and non-uniform distributed load, meaning that the uniform distributed load is defined by an even load for the entire length of the beam. Whilst the non-uniform distributed load varies throughout the entire length of the beam. Theoretically, the beam's end supports can be divided into three types: roller, pin and rigid (as graphically presented in figure 2.6). The end supports of a beam play a crucial role, especially in practice; this is because the beam's bending stresses will differ depending on what type of support it has, as a result of the deflected shape.

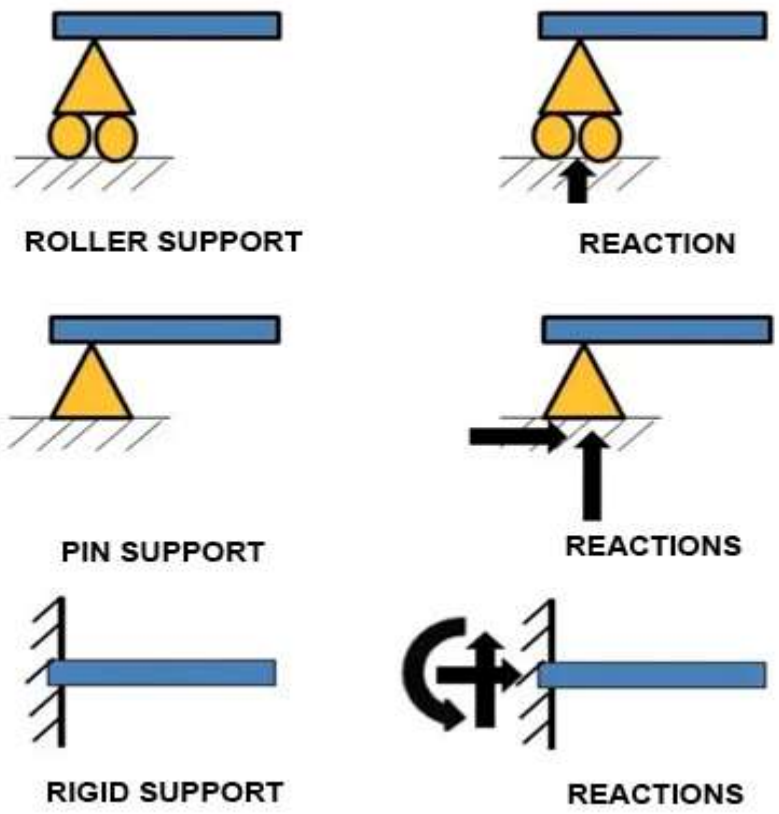

Figure 2.6 | Different types of end supports and their reactions (Popov, E.P. 1998)

As previously stated, when a load is applied to a simply supported beam, the beam experiences bending. Bending results in the formation of stresses: transverse shear and normal tension-compression. These internal forces cause the beam to deform. In fact, the internal reactions of shear force and bending moment in the application of station equilibrium are the direct source of the deformation. The bending moment of a beam is a measure of the internal forces that cause a beam to bend. This moment can either be positive or negative, depending on the curvature of the beam, which consequently depends on the direction of the applied load (Figure 2.7). (Philpot, T.A. 2019)

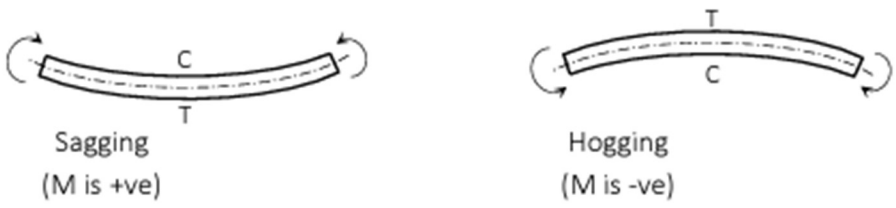

Figure 2.7 | Sagging and hogging moments (Philpot, T. A. 2019)

The design criteria of a structural steel beam is dictated by EN1990-1:2002, established serviceable limit state; which defines the deflection, and in return the bending resistance required. Therefore, the design process entails the analysis of the shear force and the bending moment.

For the purpose of this research, the end supports are designed to be simply supported so as not to create a restraining couple. As a result of this, it is the type and the position of the applied load beam that dictates the bending plane of the beam.

2.4.2 Pure Bending Of Straight Uniform Beams With One Axis Of Symmetry *(Euler-Bernoulli Theory)*

In its basic essence, the following bending theory can be easier manifested by considering the steel beam section as parallel longitudinal fibres.

The elastic beam theory is based on a number of assumptions:

1. The beam material is a homogenous and an isotropic one.
2. The beam has a plane of bending that is also symmetrical in the XY plane. After the loading is removed, this cross-sectional plane returns to its original position.
3. In the XZ plane, the beam has another plane which is the neutral axis. On this plane there is zero longitudinal strain. The neutral axis is also the plane that splits the region of compression from the region of tension. The intersection between the neutral axis and the plane of bending is known as the beam's axis.

4. The material exhibits a linear stress-strain relationship in accordance with Hooke's law within the considered loading range.
5. Young's Modulus of Elasticity, E, is identical irrespective of whether the beam is in compression or tension.
6. The beam experiences only pure bending, indicating an absence of shear forces or torsion.
7. Given that the beam's length significantly exceeds its width and depth, lateral strains, influenced by Poisson's ratio, are minimal and can generally be disregarded. (Hearn, E.J. 1997)

The FUNDAMENTAL EQUATION OF BENDING:

$$\frac{M}{I} = \frac{E}{R} = \frac{\sigma}{\gamma} \qquad \textit{Eq.4}$$

The deformed shape of the beam served as the basis for this fundamental equation, which was then completed by taking into account the moments brought about by the tensile and compressive forces away from the neutral axis[9], as well as the force equilibrium at the neutral axis. In the understanding of this subject, a comprehensive study on the full derivation of this equation would be considered to be helpful and can be retrieved from Popov (1998).

Additionally, in elastic analysis, the geometry and material behaviour are linear. Therefore, the elastic flexure formula (Eq. 4) is valid only while strain is proportional to stress. The basic kinematic assumption of the flexure theory, as stated in points 1-7, asserts the plane sections through a beam taken normal to its axis remain plane after the beam is subjected to bending. elastic behaviour is being distributed as linear stress over the cross-section and strain distribution over the cross-section. It is observed that the extreme fibres of the cross-section are experiencing the largest stresses.

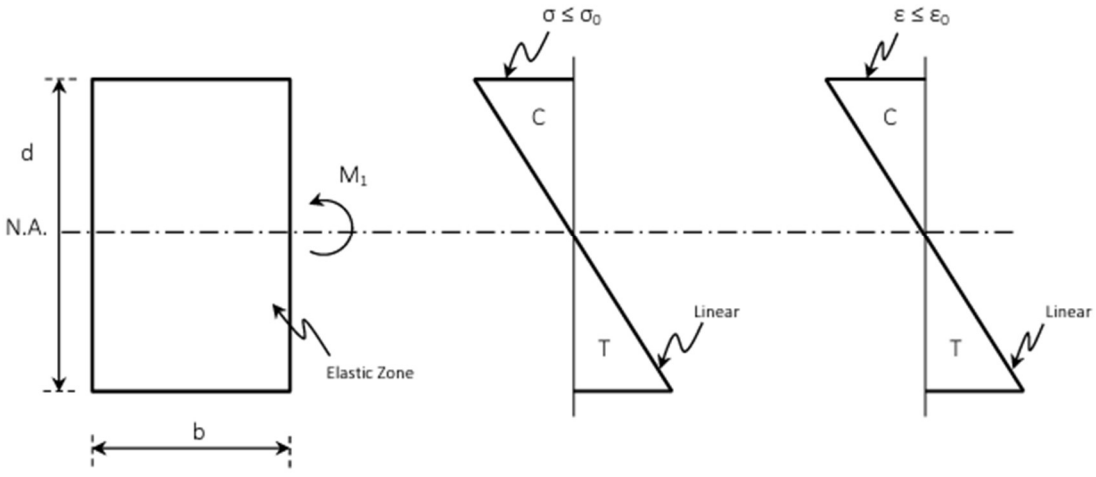

Figure 2.8 | Elastic stage cross-section, stress distribution and strain distribution (Hearn, E.J. 1997)

[9] The Neutral Axis is an imaginary line or plane that passes through the centroidal depth of the beam. It is also the plane where the beam experiences no stresses or strains.

However, when a beam is loaded beyond the elastic limit, it will start to yield. The strains at the top and bottom of the beam's fibres will finally reach the yield stress (Figure 2.8). The couple that causes the beam to start yield is known as the ***yield moment (M_o)***. (Gavin, H.P. 2015) However, even though the beam has started to yield, it can still continue carrying additional moment. The top and bottom fibres will continue to yield as the beam carries more load; ultimately, these outer-most fibres of the beam will approach the plastic zone. The beam is now considered to be in the elasto-plastic stage. The beam's curvature has changed once this point has been reached. The subsequent curvature;

$$\phi_y = \epsilon_y \times \frac{d}{2} \qquad \textit{Eq.5}$$

where is the ***yielding curvature***, $\boldsymbol{\phi_y}$.

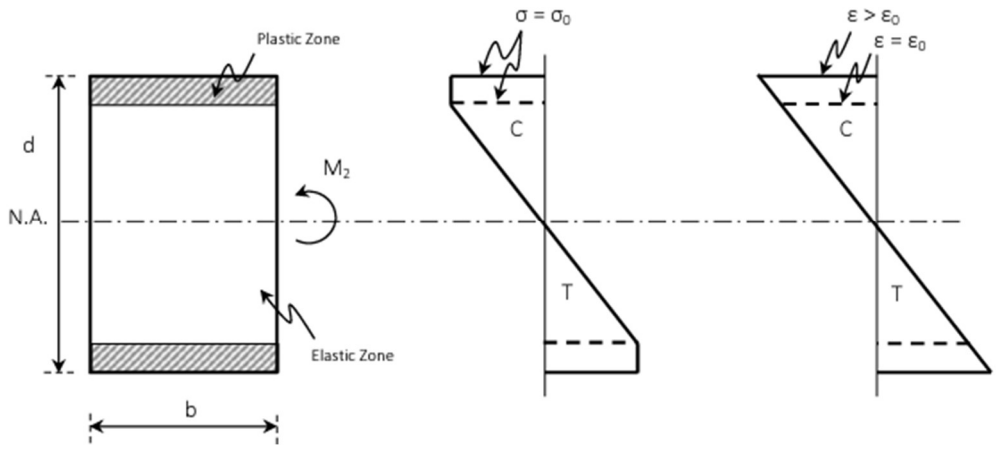

Figure 2.9 Elasto-plastic stage cross-section, stress distribution and strain distribution (Hearn, E.J. 1997)

Asymptotically, with further increase in bending moment, the beam approaches a limiting moment called the ***Plastic Moment (M_p).*** As a result, the beams can support loads in excess of what they are able to initially resist, consequently making the plastic moment always greater than the yielding moment M_o (as can be graphically presented in Figure 2.10. (Johnson W. & Mellor, P.B. 1962)

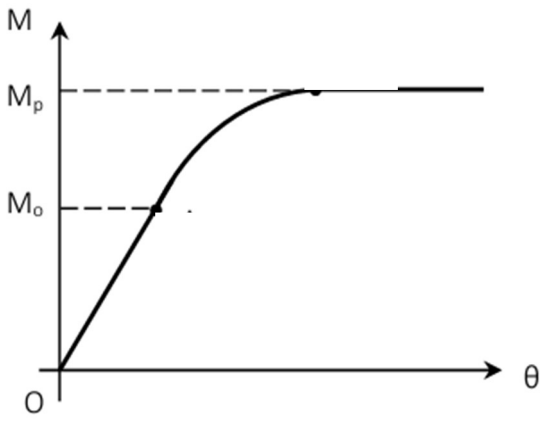

Figure 2.10 | Moment vs Stress Diagram; M_o = Yield Moment & M_p = Plastic moment (Hearn, E.J. 1997)

When all of the material of the cross-section has yielded, the section is known to be fully plastic (as shown in Figure 2.11). The maximum moment of resistance has, therefore, been reached, and as a result, a plastic hinge forms. Therefore, a plastic hinge is a point on the cross-section where it corresponds to infinite curvature. It forms at points where the cross-section is experiencing maximum bending moment. The formation of a plastic hinge results in a decrease in the structural redundancy. In the case of a statically determinate structure, an introduction of a plastic hinge renders the structure unstable (i.e. mechanism). (Johnson, W. & Mellor, P.B. 1962)

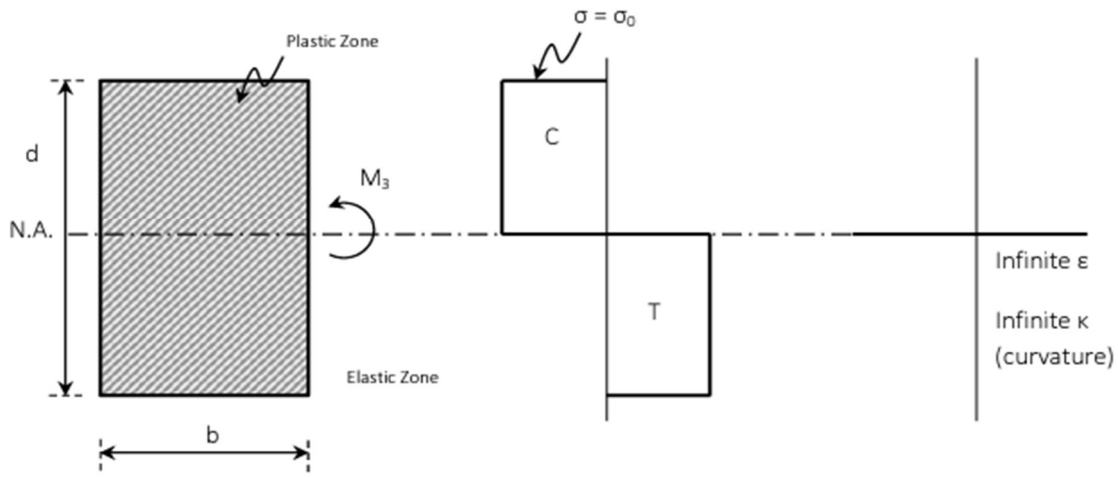

Figure 2.11 | Fully plastic stage cross-section, stress distribution and strain distribution (Hearn, E.J. 1997)

Above and below the plastic neutral axis, the plastic bending stresses are in tension and compression, respectively. The plastic neutral axis (PNA) is defined as the point in the cross-section for which the area above the neutral axis equals the area below, and as a result, the total compressive force and total tensile force must be equal to each other. (In actuality, the Equal Area Axis is another name for the P.N.A).

The plastic neutral axis and the elastic neutral axis (the centroid) are the same for symmetric cross-sections. Nevertheless, the plastic neutral axis and centroid are not the same for asymmetric cross-section.

This discussion on plastic moment capacity will clarify how it is influenced by other geometrical properties in the following chapters. Therefore, the plastic moment capacity, M_p, will be calculated in a subsequent chapter for sections that have varying geometrical properties.

From previous literature, a sensitivity analysis was conducted on beams ranging from IPE 160 to IPE 240. The findings from this analysis indicated that yield strength and flange thickness significantly influence the load-bearing capacity of a beam, as illustrated in Figure 2.12. However, it is important to

note that this research did not encompass all the geometric properties. This current research aims to bridge that gap by incorporating a broader range of geometric variables, providing a more comprehensive understanding of their impact on the ultimate flexural capacity of all section sizes. This extended analysis (that will be described in the following chapters) will allow for a deeper exploration of how each geometric dimension contributes to the plastic moment capacity. (Melcher, J. et al., 2020)

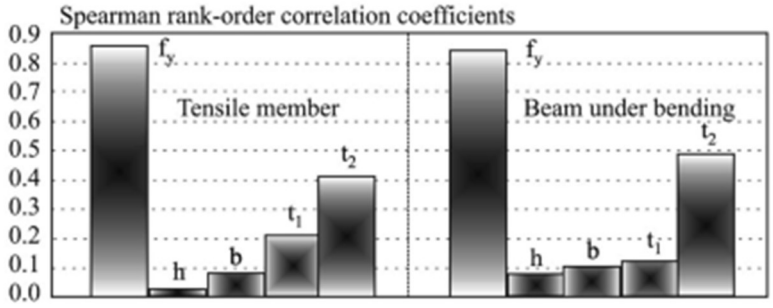

Figure 2.12 Sensitivity analysis between load-carrying capacity and dimensional influence (Melcher, J. et al., 2020)

2.5 Conclusion

In summary, steel is an essential material in engineering and construction due to its many qualities and adaptability. Steel's grade and characteristics are determined by its composition, especially by the amount of carbon present; the most commonly produced type is plain carbon steel. In engineering design, steel's mechanical characteristics—such as its yield strength, ultimate tensile strength, elastic modulus, and shear modulus—are essential for guaranteeing structural performance and stability.

The behaviour of structural elements under external loads is clarified by the study of beam bending and deflection, which helps engineers build structural sound and effective structures. An analytical framework for beam deformation and stresses is provided by the elastic bending theory of beams, which is predicated on concepts such as material homogeneity and linear stress-strain relationships. The cross-sectional area and moment of inertia of steel beams are two geometric parameters that affect bending resistance, which further informs structural design and analysis.

Furthermore, material characterisation and testing, as demonstrated by mill test reports, assures the dependability and quality of steel components by providing important information regarding the mechanical characteristics, chemical composition, and dimensional measurements of the steel component. This ensures the efficiency, durability, and safety of engineering applications. Essentially, steel's mechanical qualities and versatility make it a necessary component in contemporary engineering and construction, aiding in the creation of durable infrastructure across the globe.

3 Steel Beam Fabrication Accuracies, Design Codes, and Reliability

3.1 Introduction

Since hot-rolled sections, particularly I-profiles, have been created, they have become an integral part of a wide array of applications, especially due to their flexural performance. The I-profile is created during the rolling process, which influences the strength and geometric dimension along the y-axis. Therefore, the standardisation of these profiles has been important to maintain consistency and ensure structural performance. However, the Eurocode allows dimensional tolerances for these beams.

This chapter presents a detailed exploration of the limit state principle, as utilised by the Eurocode. This principle facilitates the determination of the probability of failure, which is also an important factor that will be tackled in the following chapter. Furthermore, the application of the limit state principle forms an essential component of the methodology employed in the analysis. With this approach, the dimensional tolerances established by the Eurocode can be analysed, and the probability of failure can be calculated.

3.2 Designation and Standardization

The widespread adoption of hot-rolled sections with I profiles across various engineering fields led to the standardization of their production early on, with predefined types and sizes being established. In 1951, the formation of the European Community on Coal and Steel (ECSC) marked the beginning of the harmonization process for hot-rolled profiles.

The unique structural properties of the I profile are closely tied to the high centrifugation of the material induced by the rolling process, as illustrated in Figure 3.1. This centrifugation results in a significant increase in the second moment of area of the section along the y-axis. “The morphological transformations, generated by the rolling process, contribute to increase the flexural performance of the structural element, modifying at the same time the structural behaviour” (Di Lorenzo et al., 2017) as the material is being divided into two zones, the central area and the two horizontal legs.

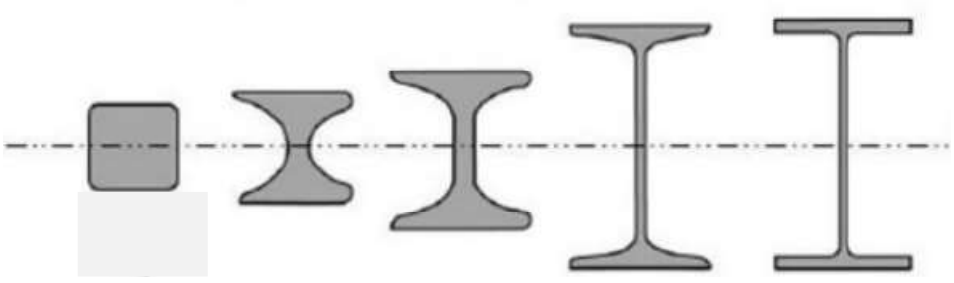

Figure 3.1 | Shape morphing during the hot-rolling process. (Di Lorenzo et al., 2017)

In practice, the dimensional tolerances for steel beams achieved during both fabrication and on-site installation can be influenced by various factors. The major factors depend on the capabilities of the fabrication facility, the expertise of workers, methods of transportation and handling, and site environmental conditions. Effective coordination and quality control measures are essential to ensure that the specified tolerances are met throughout the manufacturing and installation processes. By understanding how these dimensional tolerances are created enables a clearer comprehension of their significant role in this research. Especially since these dimensional tolerances impact the structural behaviour of steel beams, specifically their plastic moment capacity. (Byun, 2019)

3.2.1 Mill Tests

A material test report (MTR), also referred to as a mill test report, is a crucial quality assurance document issued by a manufacturer to certify the chemical and physical properties of a particular batch of material. The typical contents of a mill test report encompass:

1. ***Chemical Composition***: Detailed breakdown of the elemental makeup of the material, specifying the percentage composition of various elements present.

2. ***Mechanical Properties***: Information regarding the material's strength, hardness, ductility, and other mechanical attributes.

3. ***Heat Treatment Details***: Comprehensive account of the heat treatment processes undergone by the material.

4. ***Dimensional Measurements***: Precise measurements of the material's dimensions, including thicknesses, overall width, and length.

5. ***Testing Methods***: Explanation of the methodologies employed to assess the material's properties, ensuring thorough examination.

6. ***Compliance with Standards***: Confirmation of the material's adherence to specific industry standards or customer specifications.

In contrast to other sources of material strength data, mill tests offer a comprehensive and standardized source of information, integral to the steel production process. (Byfield & Nethercot, 1997)

3.3 Structural Design Codes

The Eurocode effort was initiated in the 1970s to eliminate the obstacle to trade across various national codes. The British Standard codes and other similar codes have a different design philosophy from the Eurocode, which uses a limit state approach. With this approach, a structure can be designed satisfactory; yet the Eurocode also suggests partial safety factors to protect and guarantee that all design structures are safe even during extreme possibilities. In Eurocodes, specifically to EN 1993-1-1 (2005), this is interpreted by the recommended numerical values of partial safety factors and other reliability parameters, present as basic values that provide an acceptable level of reliability. 'The Target reliability level and the reference period are considered as parameters and can be adjusted, so the framework remains valid under alternative economic considerations or requirements for human safety.' (Kala, 2015)

Furthermore, guidelines on steel beam tolerances are provided by EN 1993-1-1 (2005), to ensure that manufactured parts are within the necessary dimensional precision and alignment. The dimensional tolerances for hot-rolled structural steel sections are specified in EN10034 (1993), Table 1. To guarantee that the fabricated steel sections fulfil the necessary dimensional precision and alignment for construction applications, the tolerances specified in this standard are based on a quantitative study of several manufacturers demonstrates how the code permits considerable variation in the profile's width, height, flange thickness, and web thickness, all of which have a substantial impact on the profile's overall performance and structural behaviour.

Table 1 : Dimensional Tolerances for structural steel IPE sections (EN10034 (1993))

SECTION HEIGHT *h*		**FLANGE WIDTH *b***		**WEB THICKNESS *s***		**FLANGE THICKNESS *t***	
HEIGHT	TOLERANCE	HEIGHT	TOLERANCE	HEIGHT	TOLERANCE	HEIGHT	TOLERANCE
$H \leq 180$	+ 3.0 - 2.0	$b \leq 110$	+ 4.0 - 1.0	$s < 7$	± 0.7	$t < 6.5$	+ 1.5 - 0.5
$180 < h \leq 400$	+ 4.0 - 2.0	$110 < b \leq 210$	+ 4.0 - 2.0	$7 \leq s < 10$	± 1.0	$6.5 \leq t < 10$	+ 2.0 - 1.0
$400 < h \leq 700$	+ 5.0 - 3.0	$210 < b \leq 325$	+ 4.0 - 4.0	$10 \leq s < 20$	± 1.5	$10 \leq t < 20$	+ 2.5 - 1.5
$400 < h \leq 700$	+ 5.0 - 5.0	$b > 325$	+ 6.0 - 5.0	$20 \leq s < 40$	± 2.0	$20 \leq t < 30$	+ 2.5 - 2.0
				$40 \leq s < 60$	± 2.5	$30 \leq t < 40$	+ 2.5 - 2.5
				$S \geq 60$	± 3.0	$40 \leq t < 60$	+ 3.0 - 3.0
						$T \geq 60$	+ 4.0 - 4.0

3.4 Limit State Principle

A basic idea in reliability analysis, design, and structural engineering is a limit state function. It is essential for evaluating the performance and safety of structures. The relationship between loads or actions subjected to a structure is quantified mathematically by the limit state function (Eq. 9). In fact, the applied loads and the component resistance are the only two important elements taken into account by the limit state function. These are also referred to as random variables, which will be presented in further depth when evaluating the variables that affect the failure event.

In order to determine whether a structure satisfies specific safety and performance requirements, the limit state function is once again employed. These standards fall into two primary categories:

- **Ultimate Limit State (ULS)**: This is the point at which the structure experiences a total/ partial collapse due to an inability to withstand further load. For this reason, the ULS exists to guarantee that the structure yields a stiffness and capacity to withstand high intense load scenarios, including ground motion loads.

- **Serviceability Limit State (SLS):** This standard ensures that even when the building experiences a degree of deformation (damage), the functional aspect of the structure is not hindered. This limit state is utilised to verify that any deformations, vibrations, or other performance requirements are within allowable bounds.

In real life, structures are typically tested for the serviceability limit state and designed to the ultimate limit state. A mix of frequency measurements regarding the structural components and subjective judgments are used to determine the probability of a structure's limit state breach. (Melcher, R. E., 1987)

The structural element fails when the value of the load effect S, which is the outcome of the calculated load Q, exceeds the value of the resistance R.

For a basic structural element, the unknown resistance R can be represented by a random variable that is sensitive to a single known load effect S and has a known probability density function $F_R(r)$:

$$P_f = P(R \leq s) = F_R(s) = P\left(\frac{R}{s} \leq 0\right) \qquad \textit{Eq.6}$$

The equation is changed to (X) in the situation when the load effect is undetermined and is represented by the random variable S with a probability density function $F_s(S)$.

$$P_f = P(R \leq s) = P(R - S \leq 0) \qquad \textit{Eq.7}$$
$$= \int_{-\infty}^{\infty} F_R(x) f_s(x) dx$$

This is referred to as the fundamental case, assuming statistical independence between the resistance and load variables. The previous equation provides the total chance of failure product of two independent events. In Figure 3.2, the density function of R and S is plotted to better understand.

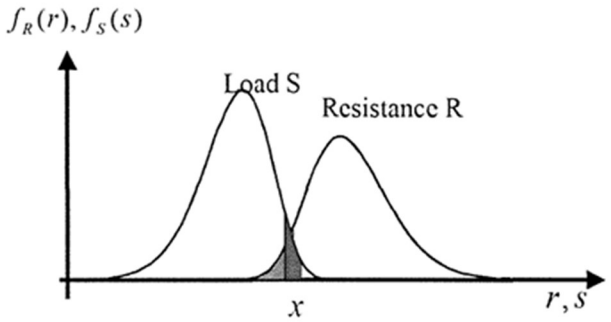

Figure 3.2 | Load and Resistance Probability Density Functions (P. Thoft-Christensen, M. Baker, 1982)

The load S and resistance curves in Figure 3.2 overlap, but this does not indicate the likelihood of failure. The integral under this density, as presented in Figure 3.3 gives the probability of failure.

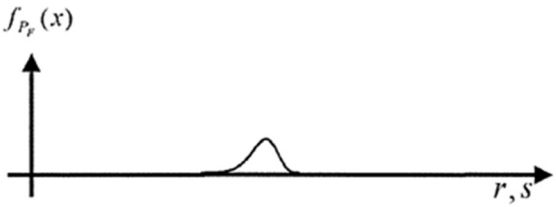

Figure 3.3 | The failure probability density function (P. Thoft-Christensen, M. Baker, 1982)

The failure probability can be written as follows when the load variable S and the resistance variable R have normal distributions:

$$P_f = P\,(M \leq 0\,) \qquad \textit{Eq.8}$$

Where;

$$M = R - S \qquad \textit{Eq.9}$$

The safety margin, denoted by M, is a normal distribution with the following parameters;

$$\mu_M = \mu_R - \mu_S \qquad \textit{Eq.10}$$

and standard deviation;

$$\sigma_M = \sqrt{\sigma_R^2 + \sigma_S^2} \qquad \textit{Eq.11}$$

The following formula can be used to calculate the probability of failure using the normal distribution function:

$$P_f = \Phi\left(\frac{0-\mu_M)}{\sigma_M}\right) = \Phi(-\beta) \qquad \textit{Eq.12}$$

The formula for the safety index is equal to:

$$\frac{\mu_M}{\sigma_M} = \beta \qquad \textit{Eq.13}$$

In Figure 3.4, is an illustration of its geometrical interpretation;

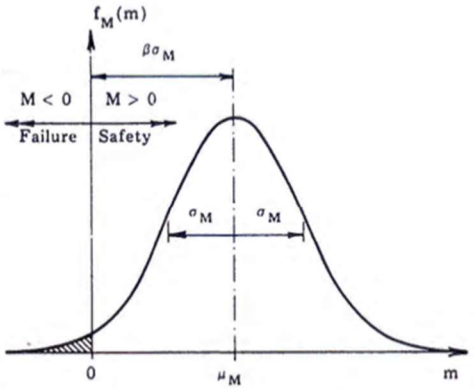

Figure 3.4 | Illustration of the reliability index (P. Thoft-Christensen, M. Baker, 1982)

It is evident that load and resistance are dependent on multiple variables rather than simply one. Therefore, these factors are mathematically described as a function of random variables as presented below:

$$R = f_1(X) \qquad \textit{Eq.14}$$

$$S = f_2(X) \qquad \textit{Eq.15}$$

Where X is a vector with n fundamental random variables (explained in Chapter 4) since R and S might not be statistically independent.

Moreover, the safety margin:

$$M = R - S = f_1(X) - f_2(X) = g(X) \qquad \textit{Eq.16}$$

is no longer normally distributed. The function g(x),is commonly used to represent the limit state function. A structural element is in the failure domain when $g(x) \leq 0$ and in the safe domain when $g(x) > 0$.

The probability of failure is calculated using the following dimension integral:

$$P_f = \int_{g(x) \leq 0} f_x(x)\, dx \qquad \textit{Eq.17}$$

When the integration is carried out over the failure domain and $f_x(X)$ is the joint probability density function for the vector of fundamental random variables X; two practical issues with this technique, nevertheless, come to light right away. Firstly, the possibility of retrieving enough data to establish the joint probability density function for the n basic variables is drastically low. Secondly, "even if the joint density function is known, the marginal densities, the multi-dimensional integration required may be extremely time-consuming." (P. Thoft-Christensen, M. Baker, 1982) In reality, these challenges can be addressed with the Level 2 methods[10] or the Monte-Carlo Simulation.

3.4.1 Random Variables

A random variable [11] is a generated or quantified value by a random event's outcome. A key concept of the probability theory regards the type of distribution of random variables as crucial as the type of distribution will provide further information about the possibility of certain occurrences happening. The central tendency and variability of these random variables' distributions can be explained by a number of characteristics, including the expected value (mean), variance, and standard deviation. There are two sorts of fundamental random variables that can be used to represent all the different types of uncertainty in an analysis: discrete and continuous variables.

- A **discrete random variable**, such as 0,1,2,3,4, etc., can have only a countable number of different values. Usually, but not always, discrete random variables are counted.

- A random variable that has an endless range of possible values is called a **continuous random variable**. Measurements are typically used as continuous random variables.

[10] Level 2 methods – A reliability method which use the mean and the variance of each uncertain parameter, together with a measure of correlation between parameters, to obtain a good approximation to the probability of failure of the component.
[11] Random variable – The variables are presented by capital letters.

3.5 Conclusion

Since the establishment of the ECCS in 1951, the use of standardised hot-rolled steel profiles—most notably, the I-beam—has had a substantial impact on engineering procedures. These profiles are widely employed in a variety of applications because of their improved flexural performance due to their features that are moulded by centrifugal forces during rolling. Tight dimensional tolerances during production are essential, necessitating close collaboration between manufacturers and strict quality control procedures.

Structural design rules, especially Eurocodes, guarantee structural integrity and safety. These codes offer detailed recommendations for material selection and building techniques. Eurocodes prioritise the use of limit states, which encompass both ultimate and serviceability limit states, and are essential for assessing structures' performance in various scenarios.

Furthermore, steel beam tolerances are specified by Eurocode 3, highlighting the significance of adhering to strict production standards to guarantee structural durability.

When evaluating the performance and safety of a structure, the concepts of limit states are essential since they take into account elements like component resistance and load effects. Quantifying uncertainties and estimating the likelihood of structural failure are made easier by the use of random variables and probability distributions.

4 Methodology

4.1 Introduction:

Nowadays, computer simulations are used extensively in research. Probabilistic simulation methods can be applied to study the effects of random variability of different quantities on the characteristics of machines, chemical or biological processes, load-carrying capacity, structural reliability, and many other contexts. One of the most effective methods for researching random processes is the Monte Carlo Simulation (MCS).

In structural engineering, the practical application of Monte Carlo simulation is evident in evaluating the performance and dependability of structures or components in unpredictable loading environments. A prime example is the assessment of the performance of structural elements such as a beam. The material's yield stress and geometrical tolerances are critical characteristics that might vary within specific ranges. These properties are modelled as random variables in the MCS, demonstrating their direct relevance and applicability in our field.

Throughout the following chapter, the study will concentrate on replicating an I-beam's behaviour while considering these random variables. The aim of using MCS was to gain insights into the probabilistic nature of the beam's performance with various geometrical tolerances and yield stress.

Towards the end of the chapter, the limit state will be used to examine how the simulated random variables affect the beam's flexural plastic capacity. In fact, the new plastic moment capacity will be investigated after considering the unpredictability brought about by the random variables with the nominal plastic capacity of the beam, which will be computed using deterministic assumptions.

With this comparison, the beam design's resilience to uncertainties can be evaluated. Hence, by combining MCS with the principle of the limit state, the probability of failure of the beam as a function of standardized geometrical and material tolerances can be analysed.

4.2 Principle of Monte Carlo Simulation

A statistical method for comprehending the influence of risk and uncertainty on forecasting and predictive models is MCS. The process starts by precisely defining and characterizing the issue or system that has to be studied, making sure that the scope, parameters, and performance criteria are all known. The input variables that affect the system are then identified, as are the corresponding probability distributions for them. These determinations can be made using theoretical arguments,

historical data, or expert opinion. Random samples of the input variables are then created after these variables and their distributions are established. Afterward, simulations are performed on these samples, enabling the execution of a large number of simultaneous calculations. Ultimately, these simulations' outputs are combined and examined, creating probabilistic forecasts. (Weinzierl, 2000)

However to further explain the MCS, a practical use of the simulation is presented. Investment firms use MCS to evaluate the risk and return of their portfolios. Using statistical models and historical data, the simulation creates hundreds of potential future states for the market. For example, by taking a random sample from the probability distributions of returns for each asset in the portfolio, an investment firm can model the performance of the portfolio in the future. These simulations account for a number of variables, including correlations between factors like asset price volatility and correlation between assets and economic conditions. By executing these simulations, the company can calculate the probability of various portfolio return levels and, additionally, the chance of substantial losses. (Rubinstein & Kroese, 2008)

The following sub-chapters will further define the main principle of the Monte Carlo Simulation, namely;

- Identifying and defining the problem
- Determination of input variables
- Generation of Random variables
- Formation of the Limit State Principle

4.3 Random Numbers

In order to simulate stochastic processes that occur in both artificial and natural environments, random numbers are needed to generate the environment itself. In fact, it is the random numbers that influence the system that is being studied, especially in simulations such as the Monte Carlo simulation. However, the challenge lies in generating these random variables in an unbiased manner. Gentle (2003) explains that even computers can never technically produce random numbers as an algorithm is required to select a random number from a range, resulting in what are known as pseudorandom numbers. However, this limitation does not hinder the statical applications, as long as the numbers appear to be drawn randomly from a specific range, it is sufficient for the purpose of the study.

In this particular study, the geometric and material properties form the random variables. As it will be further explained; such variables are crucial to the simulation study as they dictate the beam's flexural capacity.

4.4 Defining the problem

For this study, the primary focus revolved around the tolerances of a steel IPE beam and how these tolerances influence the plastic moment capacity. As already stated, the plastic moment capacity represents the maximum moment a beam can sustain once it has fully yielded across its entire cross-section. This capacity was determined using the following equation;

$$M_p = Z \times f_y \qquad \textit{Eq.18}$$

In this research, the plastic moment capacity was described as the Nominal Plastic Moment Capacity. Therefore, the beam that had the nominal plastic moment capacity had to have the ideal geometrical properties as per the design specifications. However, in practical scenarios, variations in these geometrical properties can significantly influence the actual plastic moment capacity.

Apart from the yield stress, the plastic moment capacity plays a significant factor role in the plastic section modulus (Z), which is another crucial key variable contributing to this capacity. The plastic section modulus provides a measure of the strength of the beam section when it has fully yielded. (Equation 19) Subsequently, the following variables influence the plastic section modulus: flange thickness (t_f), web thickness (t_w), height of section (h), and width of the section (w_s). Therefore these factors were taken into consideration due to manufacturing tolerances or material inconsistencies, the actual plastic moment capacity will differ from the nominal value.

$$Z = w_s \times t_f\,(h - t_f) + \left(\frac{h}{2} - t_f\right)^2 t_w \qquad \textit{Eq.19}$$

However, the equation did not take into account the root radii areas, thus reducing the flexural plastic moment capacity of the beam section. For this reason, and in order to maintain consistency with the value of the Steel Blue Book, the equation was amended to consider such aspect.

Interestingly, the Euronorm EN10034 (1993) does not provide any tolerances for the root radii. This implied that a constant (nominal) value for the radii had to be maintained in the flexural capacity calculator and is graphically presented in Figure 4.1.

$$\text{Area of ¼ circle} = ¼\,\pi r^2 = A_1 \qquad \textit{Eq. 20}$$

$$x_1 = y_1 = \frac{4r}{3\pi} \quad \textit{Eq. 21}$$

Area of square = $r^2 = A_2$ *Eq. 22*

$$x_2 = y_2 = \frac{r}{2} \quad \textit{Eq. 23}$$

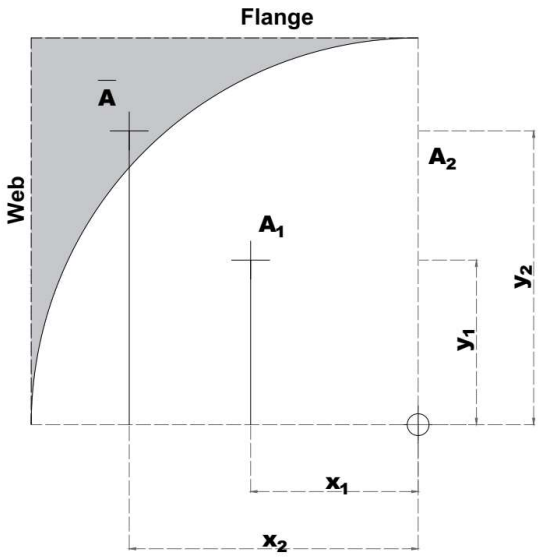

Figure 4.1 Graphical interpretation of root radius centre of rotation (Author, 2024)

For shaded area:

$$\bar{A} = A_2 - A_1 \quad \textit{Eq. 24}$$

$$= r^2 - \frac{\pi r^2}{4} \quad \textit{Eq. 24.1}$$

$$= r^2\left(1 - \frac{\pi}{4}\right) \quad \textit{Eq. 24.2}$$

$$\bar{A}\bar{x} = \Sigma ax \quad \textit{Eq. 25}$$

$$r^2\left(1 - \frac{\pi}{4}\right) \times \bar{x} = -\frac{\pi r^2}{4}\left(\frac{4r}{3\pi}\right) + r^2\left(\frac{r}{2}\right) \quad \textit{Eq. 25.1}$$

$$\left(1 - \frac{\pi}{4}\right)\bar{x} = -\frac{r}{3} + \frac{r}{2} \quad \textit{Eq. 25.2}$$

$$\bar{x} = \frac{r}{6\left(1-\frac{\pi}{4}\right)} = \bar{y} \quad \textit{Eq. 25.3}$$

Therefore, the new equation determined the plastic moment capacity of a beam, by taking into consideration the entire geometric properties of the beam's cross-section. It had to be split into three sections; (1) the flanges, (2) the web and (3) the root radii. The explanation of how the moment occurs

about the plastic neutral axis can be found Theory Of Elastic Bending Of Beams section 2.4.2. Below is the procedure that was taken to find the plastic section capacity for beams with varying dimensional geometrical properties.

$$M_p = \underbrace{[2F_{ft} \times y_{ft}]}_{\text{Flanges}} + \underbrace{[2F_{wt} \times y_{wt}]}_{\text{Webs}} + \underbrace{[4F_{rt} \times y_{rt}]}_{\text{Root Radii}} \qquad \textit{Eq. 26}$$

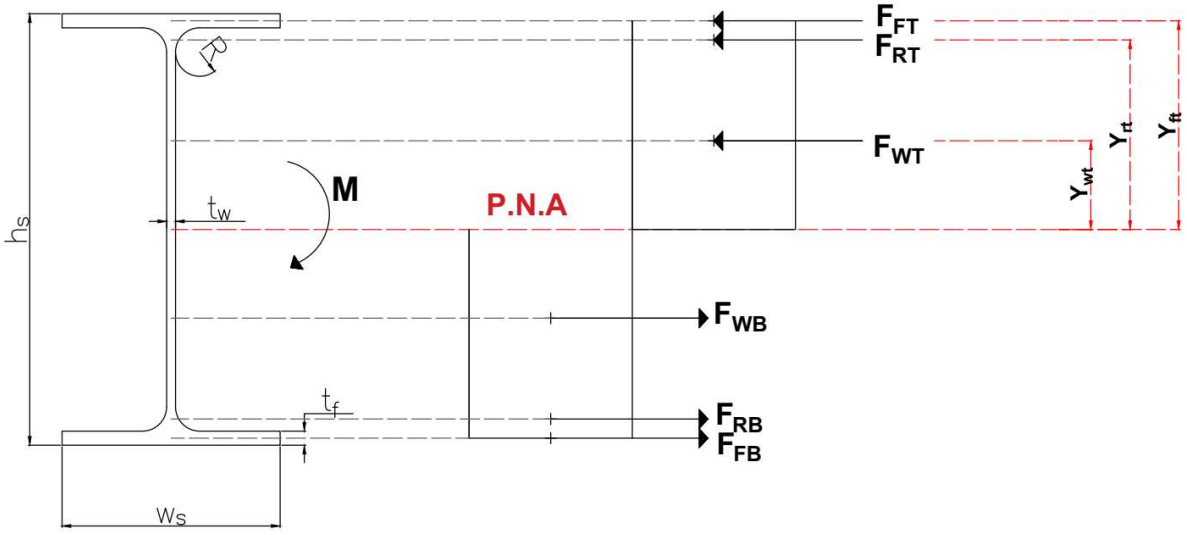

Figure 4.2 Graphical representation to determine plastic moment capacity (Author, 2024)

$$F_{ft} = (w_s \times t_f) f_y \qquad \textit{Eq.27}$$

$$F_{wt} = \left(\frac{(h-2t_f)}{2} \times t_w\right) f_y \qquad \textit{Eq.28}$$

$$F_{rt} = r^2\left(1 - \frac{\pi}{4}\right) f_y \qquad \textit{Eq.29}$$

$$y_{ft} = \frac{h}{2} - \frac{t_f}{2} \qquad \textit{Eq.30}$$

$$y_{wt} = \frac{\left(\frac{h}{2} - t_f\right)}{2} \qquad \textit{Eq.31}$$

$$y_{rt} = \frac{(h-2\,t_f)}{2} + \bar{y} \qquad \textit{Eq.32}$$

From equation 25:

$$y_{rt} = \frac{(h-2\,t_f)}{2} + \frac{r}{6(1-\frac{\pi}{4})} \qquad \textit{Eq.33}$$

Hence, in this study, the aforementioned factors—yield stress, flange thickness, web thickness, height, and width of the section—were regarded as random variables. By considering these parameters as random variables, the study aims to provide a more comprehensive understanding of the beam's plastic moment capacity.

Table 2 The random variables

VARIABLES	**X_1**	**X_2**	**X_3**	**X_4**	**X_5**
	WIDTH OF SECTION w_s	SECTION HEIGHT h_s	WEB THICKNESS t_w	FLANGE THICKNESS t_f	YIELD STRESS f_y

4.4.1 Variables on Section Members

In the computational model, the allowable variations in geometrical parameters were determined based on the specifications provided in EN 10034 (1993). Therefore, for each beam analysed, the tolerances had to be adjusted according to the limits outlined in Table 1. From this table, it was observed that as the size of the beam increases, the permissible tolerances also increase.

In order to expand the study's scope, the figures listed in the tolerance table were divided into smaller increments while at the same time maintaining the original range, with the limiting values included.

Given that the established tolerances differed for each variable, the increment step size changed based on the particular variable. This implied that the section height and the width of the flange had greater tolerances when compared to the other variables; hence, in this study, increments of 0.05mm were chosen. Smaller step increments were adopted for the flange thickness and the web thickness, which are subject to substantially smaller tolerances. This approach was implemented for two reasons: (1) to make sure that each variable's tolerance constraints were met by the increments precision and (2) to limit the probability of having duplicate generations, as this would influence the Monte Carlo simulation.

4.4.2 Variables on Material Properties

Material properties as discussed in section 2.2, are laboratory measurements, meaning that they inherently include random errors. These inaccuracies are caused by several issues, such as small calibration differences, testing apparatus misalignments, variations in chemical composition, impurity levels, and microscopic flaws. It is recognized that, in practice, no two material samples are going to be

precisely the same. In fact, it is this variability that can be statically analysed to determine the likelihood of the probability of variations.

Due to its numerical magnitude, the main material property that influences the plastic moment capacity (as can be seen from equation 18) is the yield stress. For the purpose of this study, only mild steel was considered. The mean [12] and standard deviation[13] of mild steel were defined, and from this established standard deviation mean, a range was decided upon. The range allowed for a high degree of confidence in material performance, yet at the same time, it had been established with scientific rigor. This justified the choice of the range of the yield stress based on a systematic, quantitative analysis rather than assumptions.

Below is the procedure for finding the mean and two standard deviations from the mean, which was used to establish the range for the yield stress.

$$S_{o.charc} = S_{o.\ Mean} - k\ S_{o.stand.dev} \qquad \textit{Eq. 34*}$$

$$S_{o.COV} = \frac{S_{o.stand.dev}}{S_{o.Mean}} \qquad \textit{Eq. 35}$$

$$S_{o.stand.dev} = S_{o.COV} \times S_{0.Mean} \qquad \textit{Eq. 35.1}$$

Therefore substituting equation 35 into equation 34:

$$S_{o.charc} = S_{o.\ Mean} - 1.65 S_{o.COV} \times S_{o.Mean} \qquad \textit{Eq. 36}$$

$$S_{o.charc} = S_{o.\ Mean} \times [1 - 1.65 \times S_{o.COV}] \qquad \textit{Eq. 36.1}$$

** k = 1.65 for a normally-distributed uncorrelated basic random variable and a 5% fractile* (Swift et al., 2010)

Since;

$S_{o.charc} = 275 N/mm^2$

Assuming that $S_{o.COV}$ is 7%, then;

$S_{o.COV} = 0.07$

[12] Mean: The mean provides a central value for the data set, representing the average yield strength of the mild steel.

[13] Standard deviation: This static measures the amount of variability or dispersion from the mean.

Substituting into equation 35;

$$275 = S_{o.\,Mean} \times [1 - 1.65 \times 0.07]$$

$$S_{o.\,Mean} = \frac{275}{0.8845} = 310.9101 \text{ N/mm}^2$$

Therefore, the standard deviation can be found with equation;

$$S_{o.stand.dev} = S_{o.COV} \times S_{o.Mean}$$

$$= 0.07 \times 310.9101 = 21.7637 \text{ N/mm}^2$$

Now determining two standard deviations away from the mean from both ends:

$$S_{o.Mean} - [2 \times 21.7637] = 267.3827 \text{ N/mm}^2 \approx \mathbf{270\ N/mm^2}$$

$$S_{o.Mean} + [2 \times 21.7637] = 354.4375 \text{ N/mm}^2 \approx \mathbf{355\ N/mm^2}$$

With these values, a range for the final variable considered within the Monte Carlo simulation had been set up. The lowest value was 270, and the greatest value was 355, with increments of 5N/mm^2.

4.5 Generation of combinations

For the Monte Carlo simulation, the generation of random variables was conducted through Microsoft Excel's Visual Basic Application, also known as VBA. VBA allows users to program algorithms and automate processes. With the use of an algorithm presented in Appendix A1, a large number of randomly selected variables were chosen from a range, which allowed the production of a broad number of scenarios systemically. These scenarios were coded to randomly select a variable from a range that was established depending on the Euronorm, EN10034 (1993).

However, the number of runs generated was determined through a test that was carried out prior. For instance, the five variables in the I-section IPE360 each had a unique number of ranges. For the MCS, it is important that all combinations generated are unique, meaning that each variable is unique within a combination. Therefore, since each random value can be repeated independently, it was important to check for duplicate combinations within the Excel sheet.

Below is a representative example illustrating the number of combinations required to ensure that every possible variable is paired with each other, resulting in all unique runs.

-Var X_1 : 121 possible values

-Var X_2 : 121 possible values

-Var X_3: 201 possible values

-Var X_4: 301 possible values

-Var X_5: 18 possible values

Therefore, the total number of combinations is the product of the variable's possible amount;

Total Number of unique equations = Var X_1 x Var X_2 x Var X_3 x Var X_4 x Var X_5

= 121 x 121 x 201 x301 x18

= 15,944,312,538 number of unique runs

Due to time limitations, a smaller number of generations was determined to be sufficient by running one test for 20,000 samples. Throughout the test, results for 100,200,500,1000,2000,10000,15,000,20000 generations were studied. The results of 2000 samples were deemed sufficient as the results had reached an asymptote, and the results' accuracy was within the region of $\pm 3\%$.

4.6 Application of the Limit State Function

From the previous chapter, the limit state function was presented as;

$$M = R - S$$

For the purpose of this study, the S was regarded as the nominal plastic section capacity, and it was determined using the Steel Bluebook. Whilst the R was the plastic section capacity with material and geometrical properties depending on which variable / test was being carried out. Therefore, M was distinguishing whether the beam with modified dimensional tolerances and/or material properties reached the nominal flexural capacity. If not, this beam M will result in a negative value, which was regarded as a failure.

The RStudio (RStudio Team, 2020) was used to generate scatterplots of these datasets. As previously mentioned, Microsoft Excel was programmed to assign a "0" or a "-1" based on whether the beam met the nominal plastic section capacity or not. The colour of the sample dot was then set to indicate if the sample passed or failed. Although it was possible to include all variables in a single scatterplot, omitting certain variables from specific plots enhanced readability and clarity. Nonetheless, to fully understand how one variable is influencing the probability of failure against the other variables, multiple tests had to be conducted as listed below in Table 3.

Table 3 Description of the tests being conducted

Test 1	All geometric variables and yield stress are randomly generated.
Test 2	All geometric variables are randomly generated with a ***constant nominal yield stress (S275)***.
Test 3	All geometric variables and yield stress are randomly generated with a ***constant nominal section height***.
Test 4	All geometric variables and yield stress are randomly generated with a ***constant nominal section width***.
Test 5	All geometric variables and yield stress are randomly generated with a ***constant nominal web thickness.***
Test 6	All geometric variables and yield stress are randomly generated with a ***constant nominal flange thickness.***
Test 7	All geometric variables are randomly generated with a ***constant nominal section height*** and a ***constant nominal yield stress (S275)***.

Test 8	All geometric variables are randomly generated with a ***constant width of section*** and a ***constant nominal yield stress (S275)***.
Test 9	All geometric variables are randomly generated with a ***constant nominal width of section*** and a ***constant nominal yield stress (S275)***.
Test 10	All geometric variables are randomly generated with a ***constant flange thickness*** and a ***constant nominal yield stress (S275)***.
Test 11	All geometric variables are randomly generated with a ***constant nominal section height*** and a ***constant nominal yield stress (S275)***.
Test 12	All geometric variables are randomly generated with a ***constant nominal section height*** and a ***constant nominal web thickness***.
Test 13	All geometric variables are randomly generated with a ***constant nominal section height*** and a ***constant nominal flange thickness***.
Test 14	All geometric variables are randomly generated with a ***constant nominal width of section*** and a ***constant nominal web thickness***.
Test 15	All geometric variables are randomly generated with a ***constant nominal width of section*** and a ***constant flange thickness***.
Test 16	All geometric variables are randomly generated with a ***constant nominal flange thickness*** and a ***constant nominal web thickness***.

It is important to note that the primary dataset, using the MCS was created primarily for Test 1. This dataset was kept consistent for the subsequent tests, with the only modification being the adjustment of one variable to its nominal value as specified in the description of each test. Additionally, these tests were applied to different section sizes (IPE 80, IPE160, IPE 240, IPE360, IPE450, IPE600 and IPE750X173) to establish whether the behaviour of the dimensional variables influenced the ultimate flexural capacity in the same manner.

Furthermore, an important aspect of the results involved comparing outcomes between different tests, specifically observing changes when one variable was kept constant in one test and two variables were kept constant in another. This procedure helped to determine the change in the probability of failure based on the variable's influence on the plastic section capacity. This comparison was facilitated by making use of the binary system that had already been established in Microsoft Excel. For example, if a sample passed in Test 2, it was marked as “0”; if it failed in Test 7, it was marked as “1”. The software

was, therefore, only programmed to highlight the differences between the tests by plotting only the changes from one test to another. Meaning that if a beam passed in both Test 2 and Test 7, it was not displayed on the scatterplot, indicating that holding the second variable constant to its nominal value did not influence the safety margin. Therefore, the new fails (sample passed test 2 and failed test 7) were denoted as "-1" and coloured in a different colour from the new passes (sample failed test 2 but then passed test 7) were denoted as "1". This is explained even further in the table below.

Table 4 Test representation of new fails and new passes

Test 2	**Test 7**	**Test 2 – Test 7**
1	0	1
0	0	0
1	1	0
0	1	-1

4.7 Conclusion

In conclusion, this chapter has explained the adequacy of a Monte Carlo simulation, especially in the context of the reliability of the I-beam's performance under varying probabilistic conditions. For this study, the simulation method has proven to be an invaluable tool with regard to assessing the resilience of the beam when subjected to random variables such as geometrical tolerances and material yield stress.

Additionally, by combining the limit state principle and the Monte Carlo simulation, a comprehensive analysis can be carried out in order to distinguish which dimensional variable is influencing the ultimate flexural capacity. It is through the comparison of the results of these tests that the influence of each variable can be studied and analysed.

5 Results and Discussion

5.1 Introduction

The following chapter is segmented into two sections, each of which focuses on a separate level of analysis to clarify the considered beams' behaviour, namely IPE80, IPE160, IPE240, IPE360, IPE450, IPE600 and IPE750x173. The first section provides a general analysis that takes into consideration all of the beams, analysing them collectively to identify any clear patterns or trends. This general analysis lays the groundwork for the second section of this chapter.

The second section of this chapter provides an in-depth analysis of three specific beams: IPE 80, IPE360, and IPE750x173. Scatterplots were used to identify any significant trends during testing. These scatterplots are instrumental as they offer visual representations of the statistical variations in the results, enhancing the clarity and understanding of the data. The adoption of these specific beams was purposely selected to create a broad spectrum of the I-sections. Therefore, with this approach, an understanding of how the dimensional variations impact the safety margin can be fully analysed.

5.2 General Analysis

The results of the probability of failure are represented below in table 5:

Table 5 | Results of the probability of failure for all tests

SECTION / TEST	IPE 80 (%)	IPE 160 (%)	IPE 240 (%)	IPE 360 (%)	IPE 450 (%)	IPE 600 (%)	IPE 750 x 173 (%)
1	3.10	6.75	5.85	9.65	7.50	6.00	9.55
2	14.35	27.10	29.50	44.75	32.80	35.55	47.45
3	3.40	7.15	6.75	10.25	7.75	6.45	9.50
4	5.30	8.45	7.00	10.30	8.00	6.05	9.60
5	3.40	6.80	5.65	9.45	7.05	6.30	9.25
6	3.60	4.15	5.40	5.80	7.05	6.90	8.15
7	15.60	29.00	31.30	46.35	34.10	36.85	47.65
8	23.40	22.15	32.25	46.50	34.30	36.00	47.95
9	14.15	27.30	29.35	44.10	32.00	35.85	47.95
10	19.75	22.65	32.15	33.25	36.10	44.35	49.65
11	5.30	8.80	7.70	11.00	8.40	6.35	9.70
12	3.40	7.40	6.60	9.90	7.80	6.75	8.90
13	3.75	5.15	6.90	7.15	8.15	7.05	8.05
14	5.10	8.60	6.45	9.80	7.80	6.05	9.15
15	7.00	7.55	6.75	7.40	8.00	6.60	8.25
16	2.90	3.40	4.85	5.85	6.60	7.05	8.00

Test 1 presents the most realistic scenario. As with the Monte Carlo simulation, the material and geometrical variables are fully randomised. The probability of failure varies between 3.10% and 9.65%, with a mean value of 7% across the range of beam sizes considered.

In this study, Test 1 suggests a relatively high probability of failure, especially when compared to the EN1990:2002 typical target failure rate for structural members, which is about 1:1000 or a target reliability index of 3.09. However, it is important to understand that the type of failure being analysed within this dissertation is different from the standard safety margin analysis.

In this context, the limit state principle has been already defined as M= R – S:

Where;

- R represents the Randomised Plastic Moment Capacity of the beam's cross-section
- S represents the Nominal Plastic Moment Capacity as derived from standard section tables.

Therefore, the study's probability of failure indicates the likelihood that the beam with the randomised properties is less than or equal to the normal plastic moment capacity.

In practice, the Safety Margin, M=R-S:

Refers to;

- R being the Randomised Plastic Moment capacity of the beam cross-section
- S being the Randomised Applied Bending Moment on the beam cross-section.

Therefore the factored safety margin, M is given by:

$$M = [\frac{R}{\gamma_m}] - [\gamma_f \times S] \qquad \text{Eq.37}$$

For onshore buildings, the Eurocode (EN1990-1: 2005) has established these partial safety factors:

$\gamma_m = 1$ and $\gamma_f = 1.35$ for Dead load and 1.50 for Live Load respectively. Assuming that 50% of the loading that causes the applied bending moment is dead load and 50% of the loading that causes the bending moment is live load, then the average value of $\gamma_f = ((1.35 + 1.50) / 2) = 1.425$.

Consequently, if the probability that the Randomized Plastic moment capacity is less than or equal to the Nominal Plastic moment Capacity is between 3.10% and 9.65%, then the actual probability of failure under factored conditions (i.e., considering the factored safety margin where the applied behind the moment is increased by 42.5%) would be significantly lower, and as a result, they would likely be closer to the target of 0.10%. This lower failure probability reflects the use and the importance of partial safety factors, which effectively increase the threshold for failure.

Thus, the probabilities of failure identified in the statistical study, while seemingly high, are not alarming. The results serve to provide a better understanding of the statistical variabilities of the allowable cross-sectional geometrical tolerances and material stress upon the plastic moment capacity of a range of steel beams subject to flexural loading. In fact, subsequent tests were necessary to gather more comprehensive data in order to be able to identify the degree of significance per variable as a function of the safety margin influence.

The general analysis continues by comparing the results of Test 1 with those of Test 2 through Test 6 to be able to establish which variable has the greatest influence on the probability of failure when randomising each subsequent parameter. From Figure 5.1 below, it can be immediately noticed that the column representing Test 2 is the most prominent, indicating the highest probability of failure. This suggests that the variability of the random variable Yield Stress is advantageous as it significantly reduces the probability of failure when compared to Test 1. This result also indicates that the dimensional properties have a great influence on the safety margin.

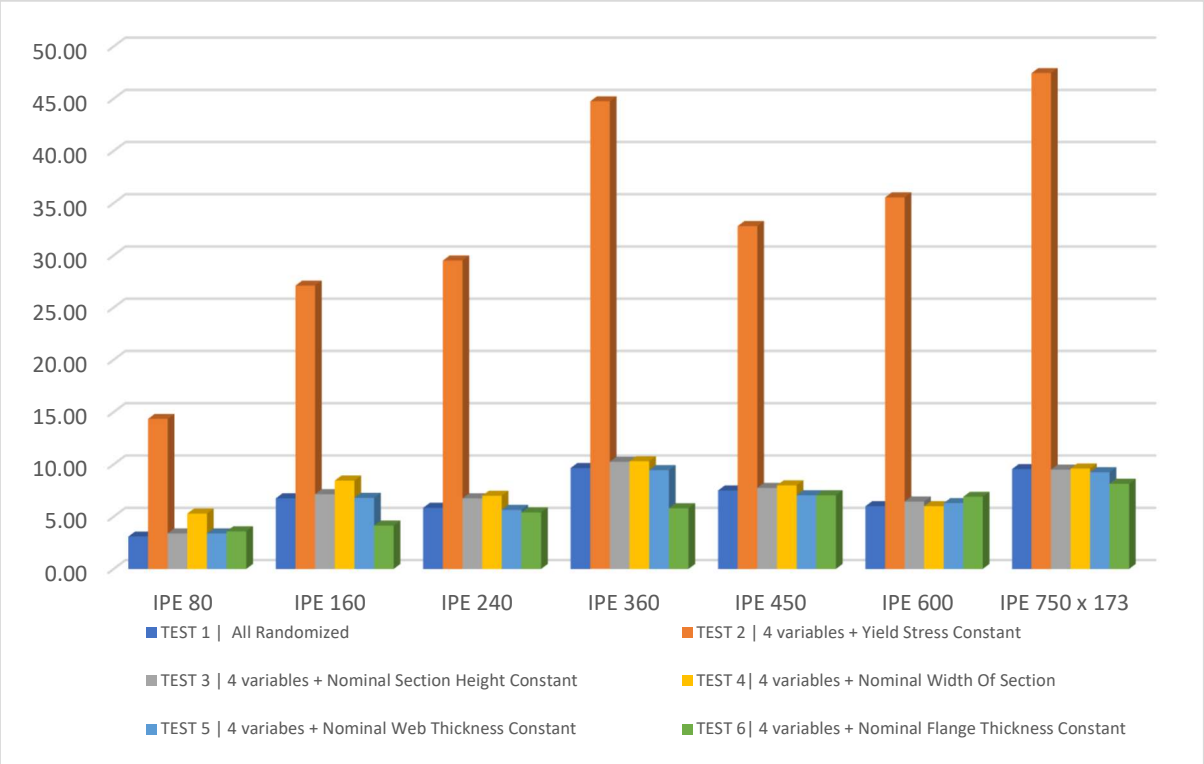

Figure 5.1 | Bar chart representing the probability of failure for test 1 to test 6

Upon comparing Test 6 with Test 1, it was observed that the variability of the flange thickness adversely affects the probability of failure; this finding is specific to the beams IPE160, IPE240, IPE360, IPE450, and IPE750x173. Conversely, for the remaining beams, IPE600 and IPE80, the variability of the flange thickness leads to a decrease in the probability of failure compared to Test 1.

Meanwhile, a consistent trend is evident from Test 4 compared to Test 1: for all beams tested, the variability in the section width reduces the probability of failure. This trend is consistent across all section sizes being tested. From Test 4, it can be concluded that for 90% of the beams, the variability of the section height slightly benefits the limit state, a minor yet noteworthy observation.

From Test 5, no discernible trend was detected. It is crucial to highlight that the variabilities of the dimensional variables are determined by the ranges established by the Euronorm, EN10034 (1993). As discussed in the previous chapter, which referenced Table 1 detailing the Eurocode's upper and lower tolerance bounds, it was noted that as the section size increases, so do the dimensional tolerances However, the results demonstrate that these tolerances do not scale linearly with section size. Further tests were conducted to observe any possible correlations between the range of dimensional tolerances for geometric dimensions of the beam cross-section and the probability of failures observed in Test 1. These tests are reported in Appendix C.6.

From Test 7 through to Test 10, where a constant nominal yield stress was maintained, together with a constant dimensional variable, it is apparent that when compared to Test 2, the most significant change in the probability of failure occurred in Test 10 (Figure 5.2). In this test, the flange thickness was held at its nominal value, highlighting that its variability has a substantial impact on the safety margin. In contrast, the other tests did not exhibit any significant changes in the probability of failure. Therefore, these results warrant detailed examination in the in-depth analysis (Section 5.3).

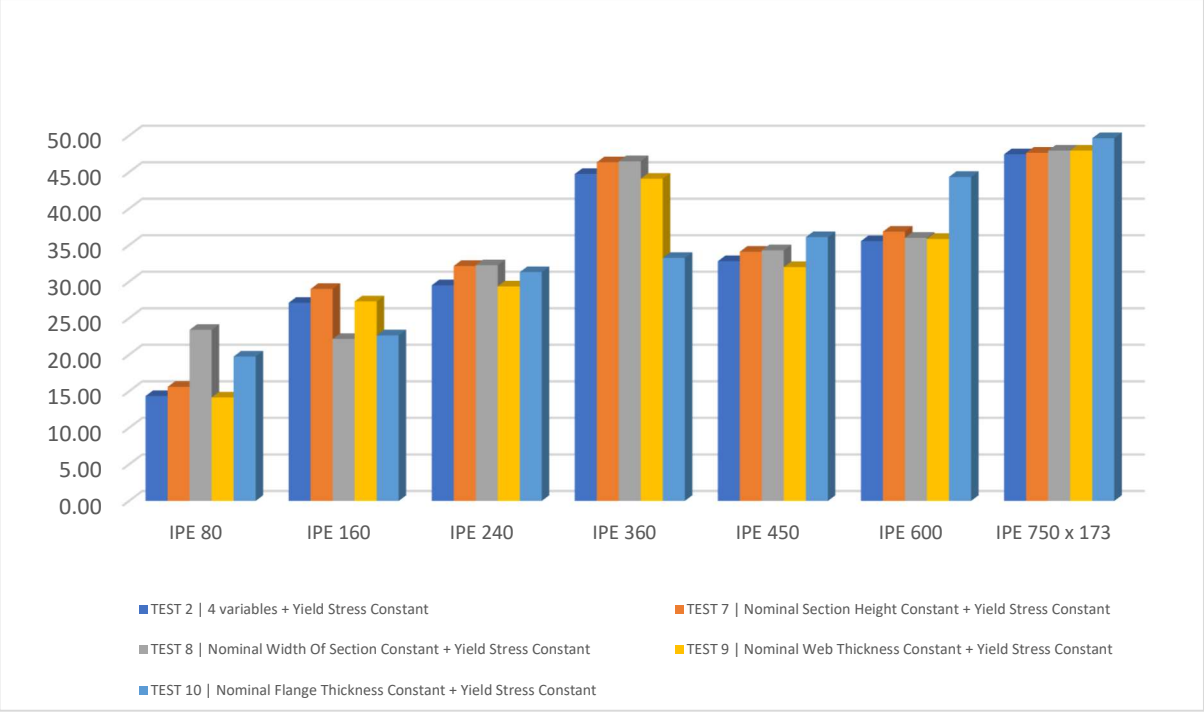

Figure 5.2 | Bar chart representing the probability of failure for test 2 and test 7 to test 10

With regards to Tests 11 to 16, the objective was to identify any significant interactions between the five variables. It was once again observed that variability in yield stress tends to reduce the change in the probability of failure. Specifically, for most of the beams (85%), when the web and the flange thickness were kept at nominal values, the probability of failure decreased when compared to Test 1. This suggested that the combined variability of these two variables adversely affected the majority of tested beams. For other variable combinations, the probability of failure changes were less pronounced, resulting in no pertinent patterns, and the responses were not consistent across all beams.

5.3 In-depth Analysis Beams IPE80, IPE360 & IPE750x173:

Table 6 Results of the probability of failure for test 1, test 2 and test 7 to test 10

	Description of test:	**IPE80 (%)**	**IPE360 (%)**	**IPE750x173 (%)**
Test 1	All Variables Randomized	3.10	9.65	9.55
Test 2	4 variables + S275 constant	14.35	44.75	47.45
Test 7	Nominal Section height + S275 constant	15.60	46.35	47.65
Test 8	Nominal Width of Section + S275 constant	23.40	46.50	47.95
Test 9	Nominal Web thickness + S275 constant	14.15	44.10	47.95
Test 10	Nominal Flange Thickness + S275 constant	19.75	33.25	49.65

5.3.1 Interpretation of Test 1 & Test 2:

As established in the previous section, Test 2 (Figure 5.6, 5.7 and 5.8) exhibited the most significant deviation from Test 1 (as graphically presented in Figure 5.3, 5.4 and 5.5) when a single variable was held constant. Consequently, these two tests are presented in scatterplots and to visually illustrate these differences the samples have been colour-coded in this manner;

- The green outline of the dot indicates that the sample has reached the safety margin.
- Meanwhile, the beams with the randomised variables that are within the safety margin are presented as a red circle.
- The internal shade of the circle depends on the third variable, meaning the colour opacity represents the size of the variable within the established range.

The scatterplots (for Test 1 and Test 2), deliberately exclude two variables for clarity purposes. By means of the general analysis, it was concluded that the variability of the section height resulted in the most insignificant geometric property. On the other hand, the randomisation of the yield stress emerged as the most prominent variable. For these reasons, these two properties were omitted in the following tests.

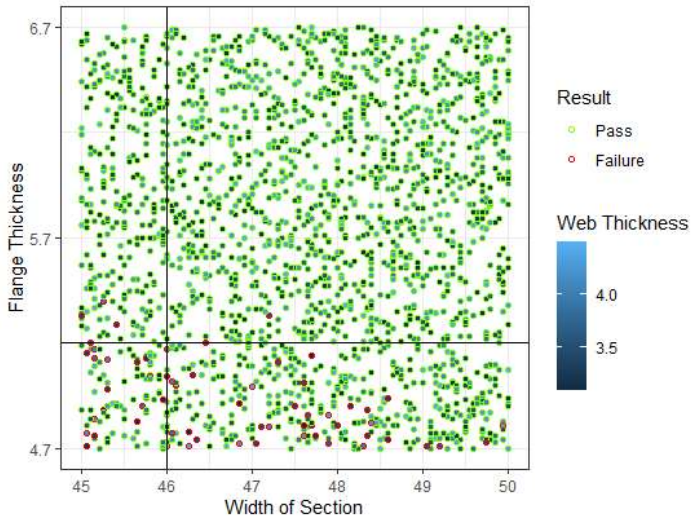

Figure 5.3 Test 1 | IPE80

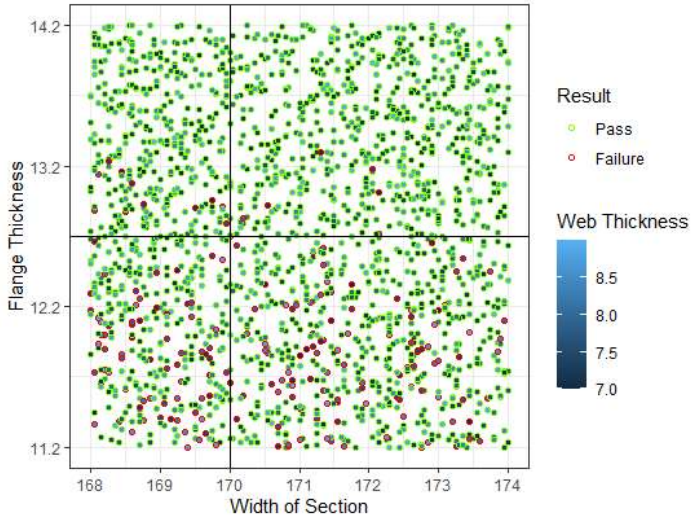

Figure 5.4 Test 1 | IPE360

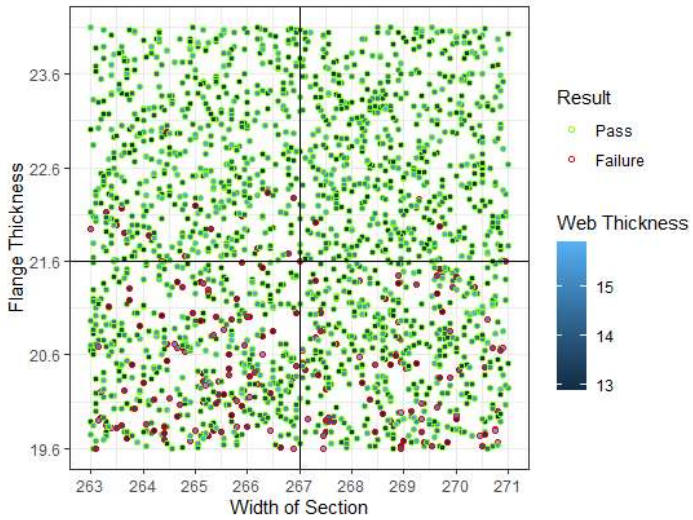

Figure 5.5 Test 1 | IPE750X173

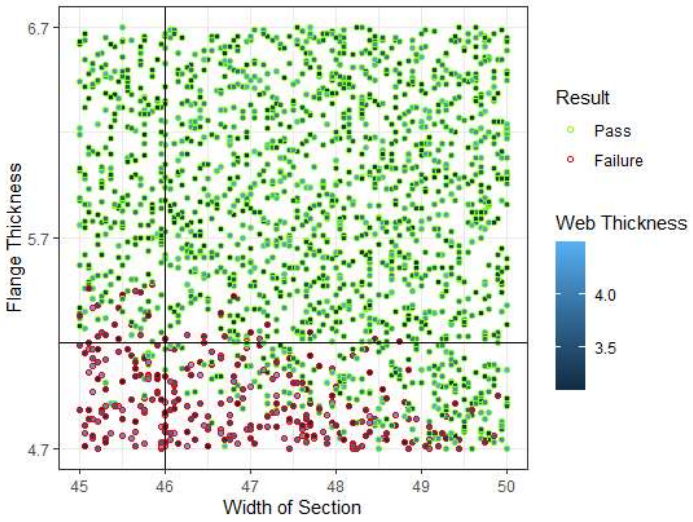

Figure 5.6 Test 2 | IPE80

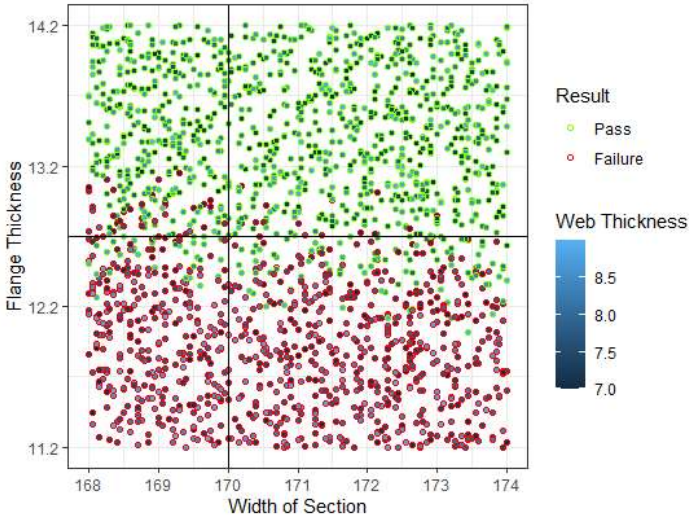

Figure 5.7 Test 2 | IPE360

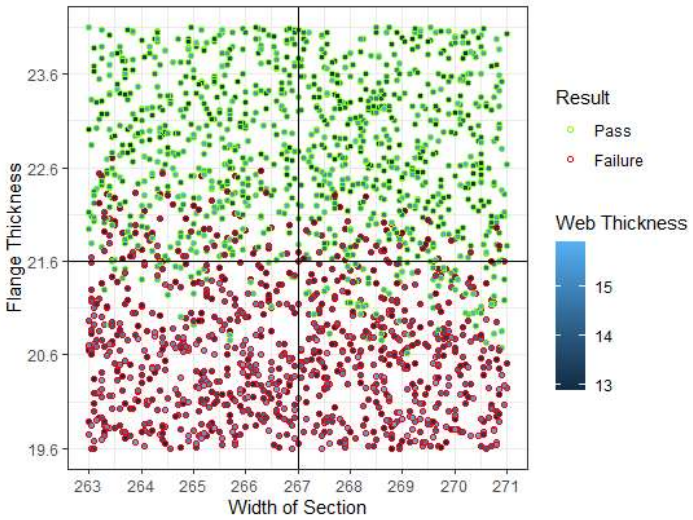

Figure 5.8 Test 2 | IPE750x173

Through Figure 5.6,Figure 5.7 Figure 5.8, a distinguishable pattern can clearly be noted. It indicates that the majority of the failed samples (88% for IPE80, 93% for IPE360, and 87% for IPE750x173) are located below the nominal flange thickness; however, since one variable is not being plotted, tests 6 through 10 can validate this observation.

The influence of the maintaining constant variable can be discerned by comparing the number of failures or new passes when the yield stress was held constant. From this scatterplot, the samples are colour-coded differently to indicate that it is a result of the difference between the two tests. Once again, the internal colour of the circle depends on the range of the third variable. Meanwhile, the outer lining of the dot depends on whether the sample has failed in either Test 1 or Test 2. In the case that the sample passed or failed both tests, this was not presented on the scatterplot, as the change in maintaining the yield stress constant did not influence the probability of failure. From these plots, it is evident that as the section size increases, the influence of the yield stress becomes more pronounced (as presented Table 7), indicating a growing importance in determining the plastic section capacity. This can be noted from Figures 5.9, 5.10, and 5.11, as the black outlined circles are more present and concentrated, whilst the pink circle dots are sparse. This is because a lot of samples had passed the randomised test and failed when they were kept constant at the 275 N/mm² value (In Figures 5.9, 5.10 and 5.11, the dots representing this information has a black outline indicating that it is a new fail.) Therefore, this exercise determined the influence of maintaining the yield stress constant. Additionally, a mathematical interpretation of the scatterplots has been established in the table below:

Table 7 Results of the probability of failure for Test 1 – Test 2

	IPE 80	***IPE360***	***IPE750x173***
New Passes (Fail Test 1 and Pass Test 2)	*4*	*14*	*8*
New Fails (Pass Test 1 and Fail Test 2)	*229*	*716*	*1226*
Samples that either failed or passed both tests	*1767*	*1270*	*766*
Total Samples Failing due to maintaining yield stress at nominal constant value for this dataset	*11.45%*	*35.8%*	*38.3%*
Total Influence on the Probability of Failure	*11.65%*	*36.5%*	*38.7%*

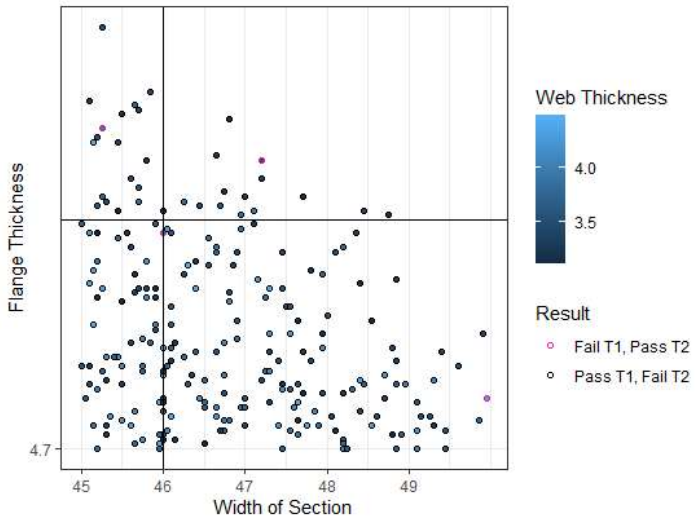

Figure 5.9 Test 1 – Test 2 | IPE80

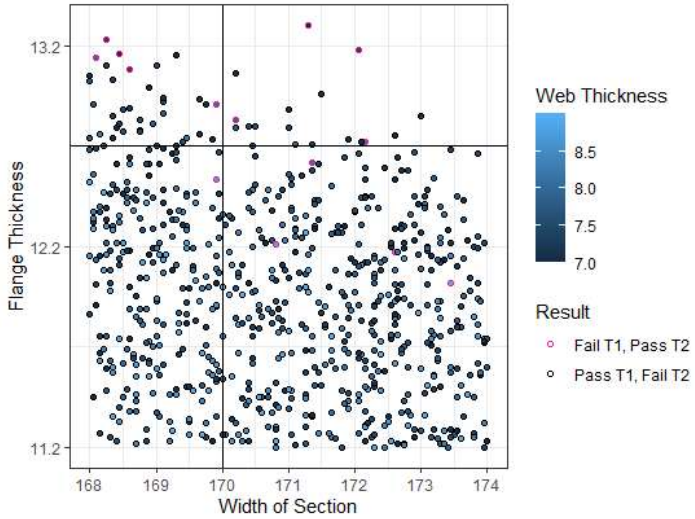

Figure 5.10 Test 1 – Test 2 | IPE360

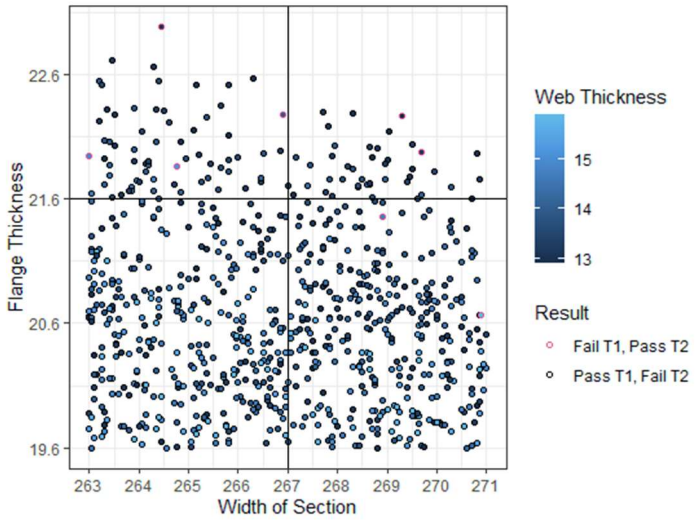

Figure 5.11 Test 1 – Test 2 | IPE750x173

5.3.2 Interpretation of Test 7 | IPE80 & IPE360 & IPE750x173:

In Test 7, both the nominal section height and yield stress are maintained at their nominal values. When compared to Test 2, where only the yield stress is kept constant, the probability of failure in Test 7 shows a slight increase for all three beams. This initiates two arguments: (1) variability in section height slightly reduces the probability of failure, and (2) it does not significantly impact the plastic section capacity.

Upon analysing the scatterplots, a graphical pattern can be established– the density of the green dots in the bottom right corner diminishes as the section size increases. This indicates that as the section size increases, the flange width becomes less significant for the safety margin. Another observation is that the samples that have a thicker flange thickness than the nominal, yet are still failing, are all marked with the darkest shade of blue inside the sample dot. This indicates that the samples fall on the smaller side of the range for the web thickness. In fact, as the section size increases, more failures are located above the nominal flange thickness line, suggesting that the variation of the two other dimensional variables can be more influential on the safety margin than the variation of flange thickness alone.

The influence of the section height can be further quantified by determining the change in the probability of failure when the section height is held constant. This observation is detailed in a graphical analysis with the scatterplots in Appendix C2. The table below summarises this analysis;

Table 8 Results of the probability of failure for Test 2 – Test 7

	IPE 80	***IPE 360***	***IPE 750x173***
New Passes (Fail Test 2 and Pass Test 7)	*51*	*23*	*29*
New Fails (Pass Test 2 and Fail Test 7)	*76*	*55*	*33*
Samples that either failed or passed both tests	*1873*	*1922*	*1938*
Total Samples Failing due to maintaining section height at nominal constant value for this dataset	*3.8%*	*2.75%*	*1.65%*
Total Influence on the Probability of Failure	*6.35%*	*3.9%*	*3.1%*

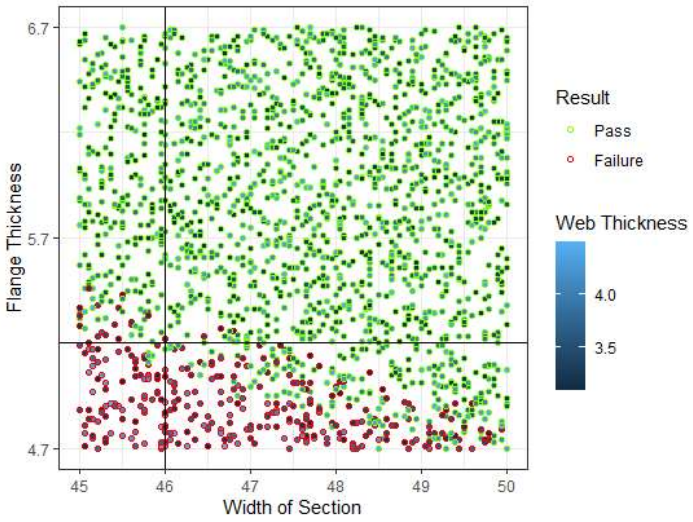

Figure 5.12 Test 7 | IPE80

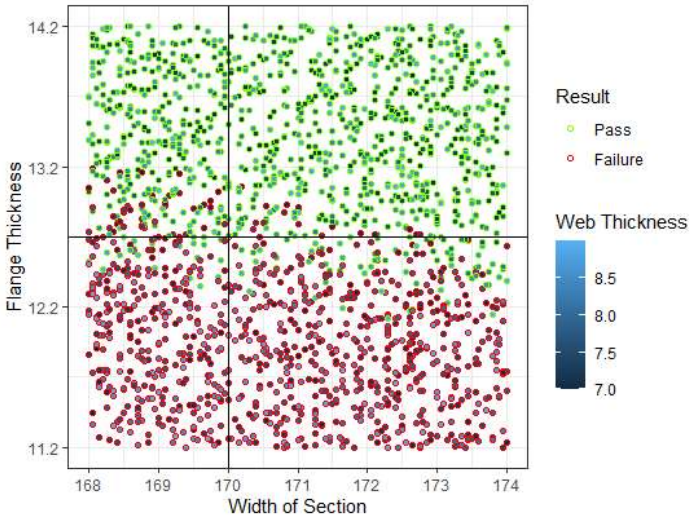

Figure 5.13 Test 7 | IPE360

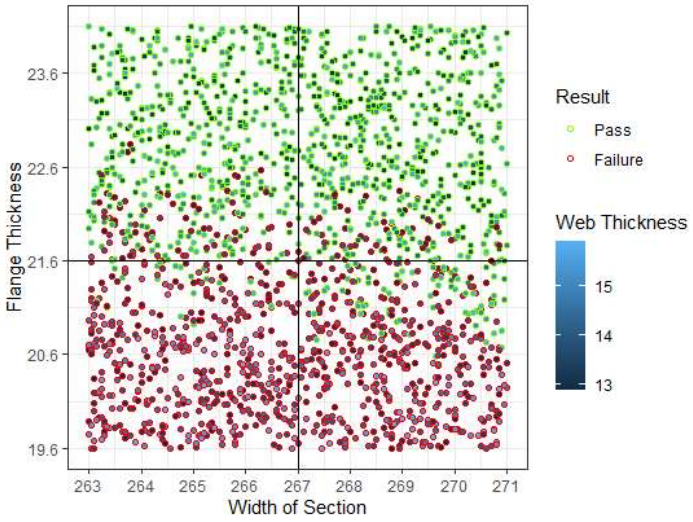

Figure 5.14 Test 7 | IPE750x173

5.3.3 Interpretation of Test 8 | IPE80 & IPE360 & IPE750x173:

During Test 8, both the yield stress and the width of the section are maintained at their nominal values. The resulting scatterplots (Figures 5.15, 5.16, and 5.17) show identical patterns to those in Test 7, reflecting the numerical similarities between the two tests. When compared to Test 2, all results from Test 8 show a slight increase in the probability of failure.

The pattern observed in the previous scatterplots was repeated here, where the majority of the failures (84% for IPE80, 93% for IPE360 and 87.5% for IPE750x173) (are situated below the nominal flange thickness line, whilst the majority of the samples that reached the safety margin are located above the threshold. From these results, it can also be noted that samples with a thinner flange thickness are passing, likely due to the fact they have a larger web thickness than the nominal. This observation was evident across all three section sizes. However, for the IPE80, the bottom left quadrant is distinctively red, indicating that even the variability of the web thickness (third variable) is not significant for smaller section sizes.

In fact, it can be concluded that as the section size increases, the influence of the variability of the section height decreases, whereas the significance of the web thickness increases. This trend indicates that the respective influence of all the geometric properties on the beam's safety margin has shifted as the section depth increases.

Appendix C3 presents the scatterplots illustrating the differences between Test 2 and Test 8. The scatterplots graphically present how maintaining these dimensional variables at their nominal values affects the probability of failure. Table 9 summarises the observed numerical data, providing a clear comparison of the impact of these tests according to the respective beam.

Table 9 Results of the probability of failure for Test 2 – Test 8

	IPE 80	***IPE360***	***IPE750x173***
New Passes (Fail Test 2 and Pass Test 8)	*16*	*25*	*34*
New Fails (Pass Test 2 and Fail Test 8)	*197*	*60*	*44*
Samples that either failed or passed both tests	*1787*	*1915*	*1922*
Total Samples Failing due to maintaining width of section at nominal constant value for this dataset	*9.85%*	*3%*	*2.2%*
Total Influence on the Probability of Failure	*10.65%*	*4.25%*	*3.9%*

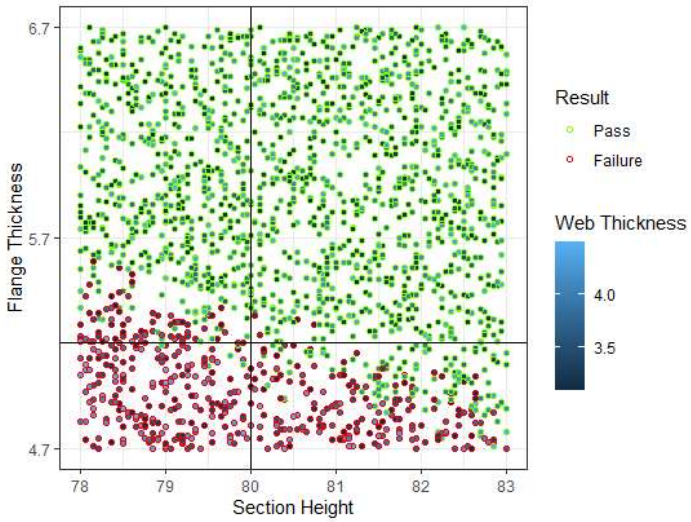

Figure 5.15 Test 8 | IPE80

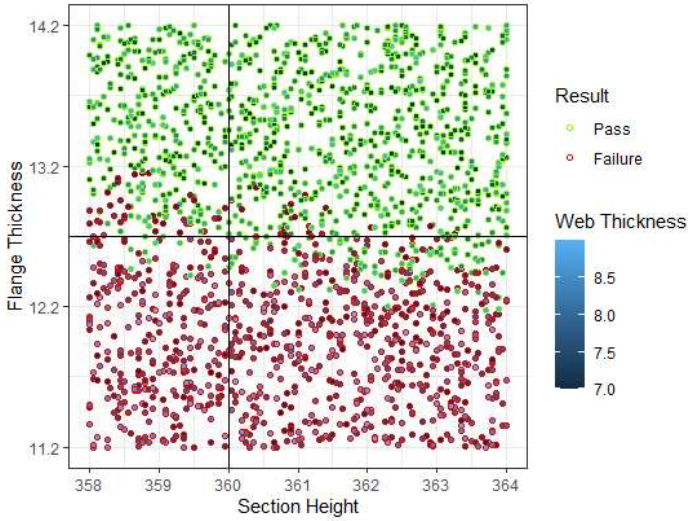

Figure 5.16 Test 8 | IPE360

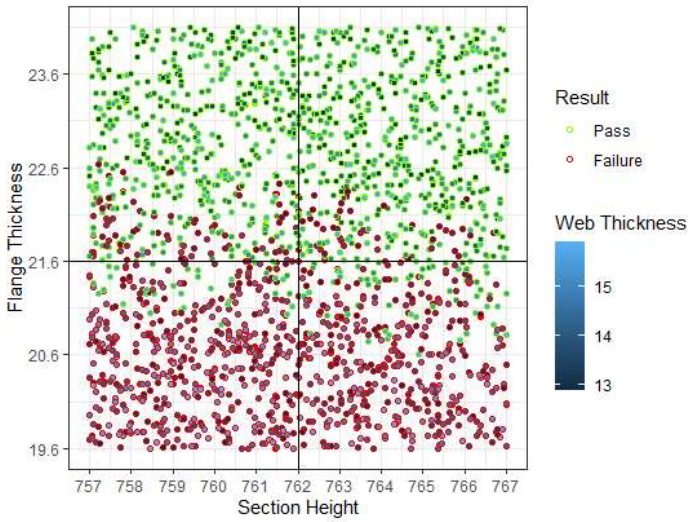

Figure 5.17 Test 8 | IPE750x173

5.3.4 Interpretation of Test 9 | IPE80 & IPE360 & IPE750x173:

In test 9, the web thickness is held constant along with the yield stress. Compared to Test 2, where this web thickness varied, the probability of failure increased negligibly. As previously highlighted, the influence of the web thickness can impact the safety margin. In fact, the results suggested that within specific ranges as a function of the section size, the inclusion of the second variable cancelled the deficiency of the flange thickness.

Therefore, by keeping this dimensional variable constant (web thickness), the other three geometric variables can be analysed. The scatterplots presented in Figures 5.18, 5.19, and 5.20 reaffirm earlier findings, highlighting that the flange thickness remains the most critical dimensional property. In fact, as the section depth increased, the horizontal line representing the nominal flange thickness became more pronounced as the failing samples established a clear division of the dataset.

From the test of the IPE 80 dataset, it was evident that the width of the section was more effective for the plastic section capacity than the section height. This was due to the fact that the samples which were located in the bottom left corner were successfully passing because they exceeded the nominal width of the section. With this observation, it was concluded that for smaller sections, the width of the section was more critical than the section height.

For larger sections, it was observed that the combination of the two-dimensional variables can influence the safety margin. This was the case with the few samples, which are located on the right-hand side and below the nominal flange thickness line, indicating that they are successfully passing due to having both dimensional variables larger than the nominal values.

Furthermore, the influence of maintaining the web thickness as a constant can be quantified by comparing samples that either fail or pass Test 2 or Test 9. These findings are all summarised in the table below, while the graphical representation of the analysis is presented in Appendix C4.

Table 10 Results of the probability of failure for Test 2 – Test 9

	IPE 80	***IPE360***	***IPE750x173***
New Passes (Fail Test 2 and Pass Test 9)	*43*	*76*	*102*
New Fails (Pass Test 2 and Fail Test 9)	*39*	*63*	*112*
Samples that either failed or passed both tests	*1918*	*1861*	*1786*
Total Samples Failing due to maintaining web thickness at nominal constant value for this dataset	*1.95%*	*3.15%*	*5.6%*
Total Influence on the Probability of Failure	*4.1%*	*6.95%*	*10.7%*

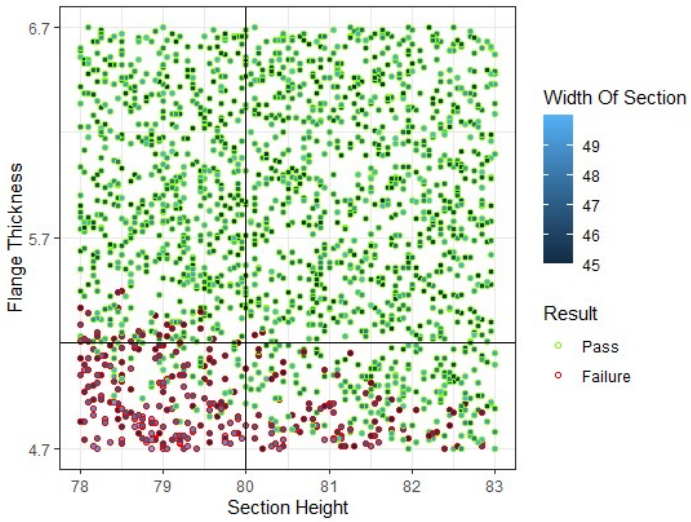

Figure 5.18 Test 9 | IPE80

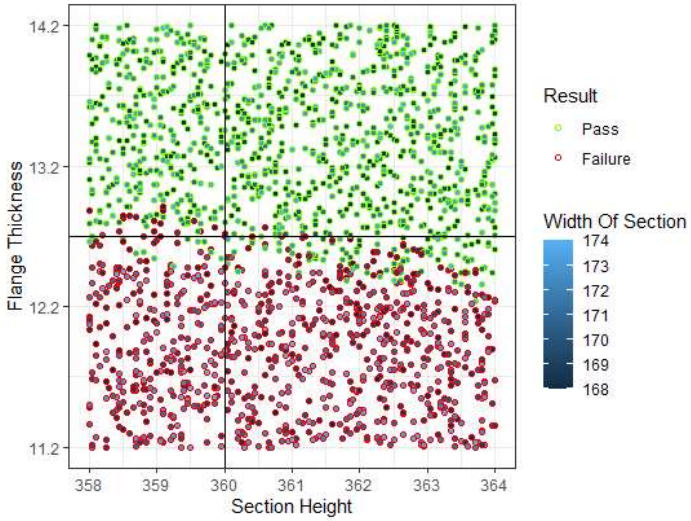

Figure 5.19 Test 9 | IPE360

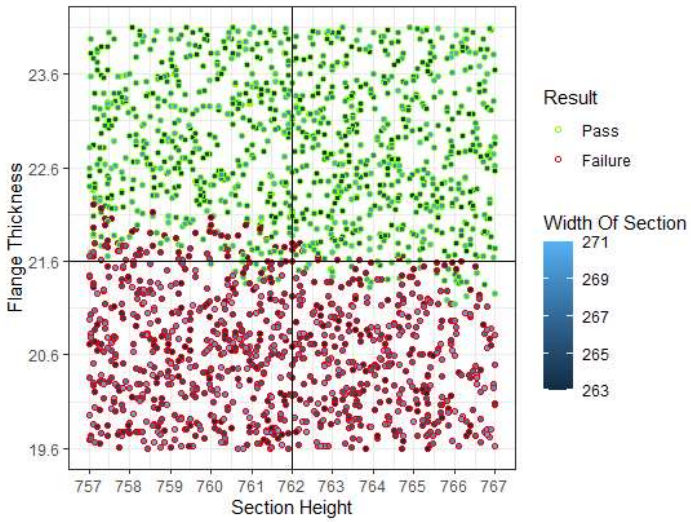

Figure 5.20 Test 9 | IPE750x173

5.3.5 Interpretation of Test 10 | IPE80 & IPE360 & IPE750x173:

Test 10 is a critical test, as already determined previous tests; the flange thickness was the most critical dimensional variable for the plastic section capacity. Therefore, by maintaining the flange thickness at the nominal value, the interaction of the three other dimensional variables was studied more comprehensively. In fact, the aim of this test was to validate all the results observed from the previous tests.

The scatterplots in Figures 5.21, 5.22 and 5.23 display a distinctive diagonal pattern, with the slope of this pattern becoming steeper as the section size increases. From the three scatterplots, it was evident that for the smaller section IPE80, there was a higher concentration of samples that reach the safety margin, unlike the IPE360 and IPE750x173. This suggests that as the section size decreases, the variability in the section width became increasingly significant over the web thickness. In fact, in Figure 5.23, it was notably apparent that the plot was divided into two sections, with very few samples exceeding the safety margin, especially those with less than the nominal web thickness. Therefore, with this test, it can be concluded that as the section size increases, both the variability of the width of the section and section height become less significant for the plastic moment capacity when compared to the web thickness.

Similar to previous sections, the analysis utilises the method of comparing the number of failures and passes between Test 2 and Test 10 to ascertain the impact of maintaining the flange thickness constant. Given that the flange thickness has already been established to be the most critical dimensional variable, this comparison quantifies the number of failures occurring due to the shift in the flange thickness. A summary of these results is detailed below, as well as in Appendix C5, where the scatterplots of this analysis are presented.

Table 11 Results of the probability of failure for Test 2 – Test 10

	IPE 80	***IPE360***	***IPE750X173***
New Passes (Fail Test 2 and Pass Test 10)	*150*	*544*	*347*
New Fails (Pass Test 2 and Fail Test 10)	*258*	*314*	*391*
Samples that either failed or passed both tests	*1592*	*1142*	*1262*
Total Samples Failing due to maintaining flange thickness at nominal constant value for this dataset	*12.9%*	*15.7%*	*19.55%*
Total Influence on the Probability of Failure	*20.4%*	*42.9%*	*36.9%*

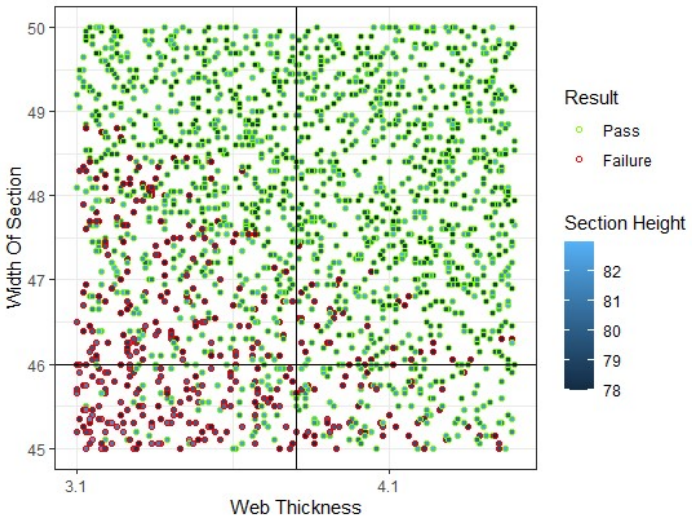

Figure 5.21 Test 10 | IPE80

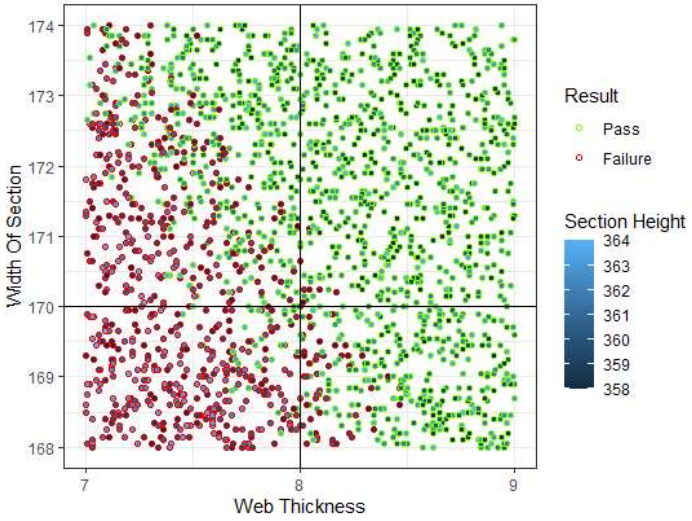

Figure 5.22 Test 10 | IPE360

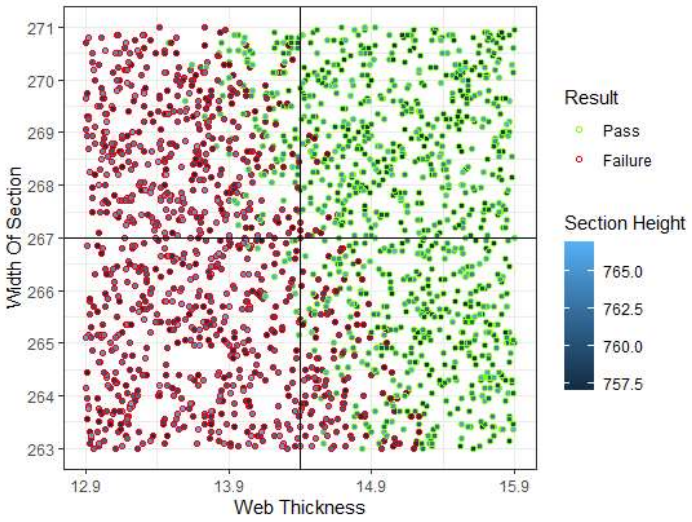

Figure 5.23 Test 10 | IPE750x173

5.4 Conclusion

The comprehensive testing carried out in this study revealed detailed insights into the probability of failure of IPE beams, with particular emphasis on the impact of dimensional and material properties. In fact, key findings across multiple tests indicated how variations in specific geometrical dimensions can significantly influence the plastic section capacity.

From Figure 5.24, it was concluded that the variability of the yield stress played a crucial role in determining the reliability of the beam in terms of ultimate flexural capacity, especially as the section depth increases. When the yield stress and another dimensional variable were kept constant, the variation in the flange thickness proved to be particularly significant, affecting the safety margins across all tests. In scenarios where both the yield stress and flange thickness were constant, the analysis of the three other geometrical variables revealed that the influence of the web thickness on the safety margin increased with the section size. Conversely, for the width of the section and section height, the influence on the safety margin decreased as the section size increased.

Therefore, it was concluded that the two major influential variables were the yield stress and the flange thickness. However, the three other dimensional variables still influenced the safety margin, as a function of the section size. Furthermore, the analysis highlighted that while the impact of single-dimensional variables like yield stress and flange thickness can be significant, the interaction between multiple variables can also control the probability of failure.

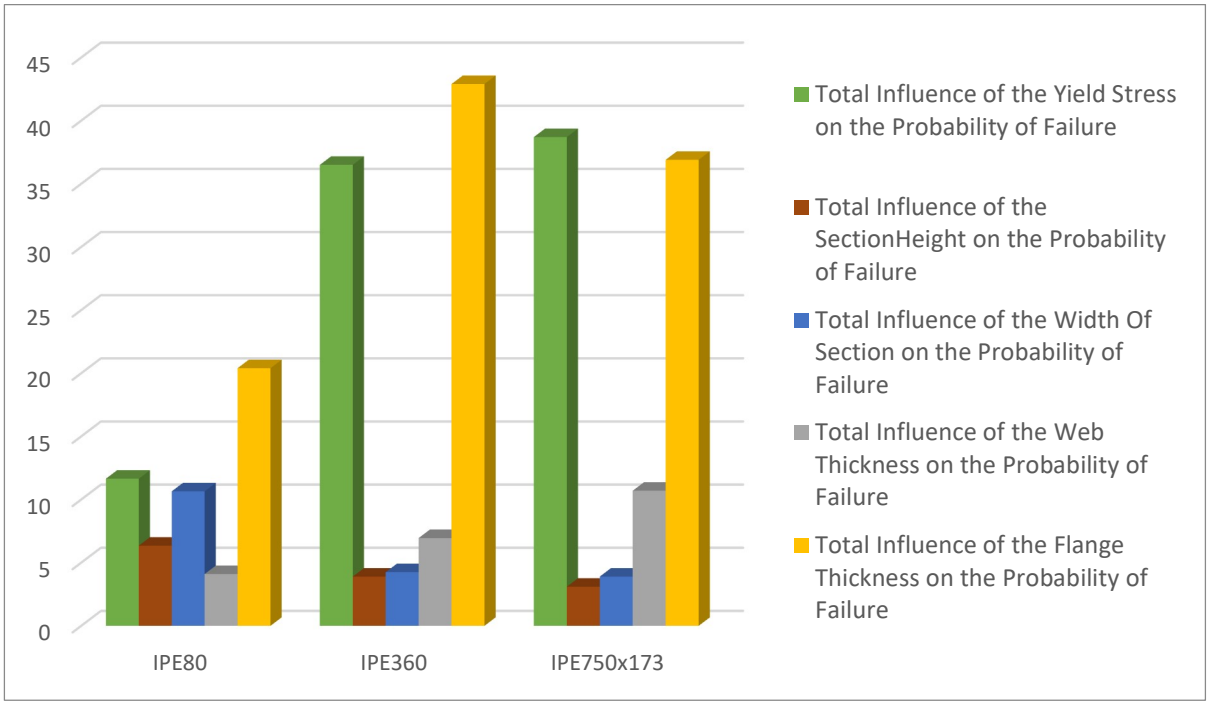

Figure 5.24 | Bar chart presenting the influence of each random variable

6 Conclusions and Further Research

6.1 Discussion

The primary focus of this dissertation was to conduct a rigorous evaluation of the effect of dimensional tolerances as established by the Euronorm , EN10034 (1993) and of random uncertainties in the material yield stress on the plastic bending moment capacity of structural steelwork beams. These tolerances, determined by the manufacturing processes are a crucial aspect of beam design. However, it is important to recognize that the ultimate flexural capacity of the beam was a result of both its geometric and material properties.

To determine the effect of each dimensional variable that the Euronorm establishes within Table 1 in EN10034 (1993), these parameters were considered as random variables. In addition, the material property, namely the yield stress, was also considered a random variable. With the utilization of the Monte Carlo simulation, the practical applicability of the range of tolerances was tested due to the fact that the Monte Carlo produced multiple realistic combinations that provided insights into the probabilistic nature of the beam's performance with various geometrical tolerances and yield stress.

The analytical method was executed using a comprehensive equation that took into account all dimensional variables as well as the root radius to calculate the plastic section modulus. These geometric variables and the yield stress were chosen at random.

The dimensional variables range was determined by the Euronorm, while the yield stress was generated randomly from a range, determined through a statistical analysis, starting with the calculation of the mean value of the yield stress. From this mean, limits were set at two standard deviations in either direction to define the boundaries of the range. With these chosen variables, the new plastic moment capacity was computed for 2000 samples per beam.

The limit state principle was also applied to establish a safety margin. This was achieved by the equation for limit state is set as M= R – S; where R is the randomised plastic moment capacity of the beam cross-section while S is the nominal plastic moment capacity of the beam cross-section obtained from standard section tables (SCI P363: Steel building design: Design data), for the purpose of this study. With this practical method in place, multiple analytical tests were conducted to determine the significance of each geometrical variable.

The most critical test for this study included a randomisation generation of all the aforementioned variables. Through this test, it was revealed that the probability of failure ranged from 3% to 9.65%. At face value, these results are of significant magnitude, especially when compared to the Eurocode's typical target failure rate 0.10% for structural members. However, it is important to consider that the

actual limit state principal takes into consideration the incorporation of partial safety factors for the applied bending moment on the beam cross-section. Therefore, these results are rather intended to enhance the understanding of the statistical variability of the allowable cross-sectional geometrical tolerances and material stress upon the plastic moment capacity of a range of steel beams subjected to flexural loading.

The limitation of the Monte Carlo simulation was its inability to determine the sensitivity factor for each variable; therefore, following test 1, an additional 15 tests were necessary for this reason. The results were subdivided into two analyses: a general study and an in-depth analysis. The general study was conducted solely at a numerical level, focusing on a quantitative evaluation of all beams. In contrast, the in-depth analysis incorporated scatterplots to visually identify any thematic trends. In fact, the latter analysis focused on 3 beams purposely selected from the range of section sizes: two from the extreme ends (IPE80 and IPE750x173) together with a mean section (IPE360). Throughout the in-depth analysis, the following significant observations that were already outlined from the general analysis were confirmed. These observations were corroborated by the interpretation of the scatterplots, which are presented below:

- The tolerances established by the Euronorm do not correspond proportionally to the section sizes, as evidenced by the results of tests where only one dimensional variable was held constant at its nominal value. No obvious pattern emerged from these tests, indicating that there are no consistent trends across all section sizes. This confirms the hypothesis that the tolerances do not increase proportionally with section sizes.

- The most prominent observation was retrieved when the material variable (i.e., yield stress) was kept constant. With this result, it was revealed that the variability of the yield stress enhanced the probability of failure. This conclusion is evident in all the tests where the yield stress maintained its nominal value, the probability of failure increased significantly when compared to Test 1 (all variables randomised). Therefore, with these additional tests, it was established that the yield stress is not only a significant factor for the plastic moment capacity, but it is also a factor that gains influence on the plastic moment capacity as the section size increases.

- From the batch of tests where the yield stress and a single geometric variable were constant (section height, flange width, and web thickness), the scatterplots highlighted a common pattern throughout. The pattern indicated that the most critical dimensional variable is the flange thickness. This observation was based on the fact that most of the samples that were

failing (approximately 89% for IPE80, 95% for IPE360 and 87% for IE750x173) were located below the flange thickness threshold.

- The combination of the variability of other dimensional variables can be as influential on the safety margin as the flange thickness. The influence of the remaining dimensional variables was not consistent throughout all section sizes. Specifically, as the section size increased, the significance of both the width and height of the section decreased by 6.75% and 3.25%, respectively. Conversely, the importance of web thickness grew by 6.6% with increasing section size. These findings illustrate that the relative importance of each geometric dimension on the probability of failure, as determined by the ultimate limit state of the plastic moment, varies across different section sizes.

6.2 Further Research

The following section proposes further research based on the study's results discussions, as well as on the limitations that were encountered throughout this study. Due to time limitations and other constraints, these research topics were not explored but might be of an added value to this area of study:

1. A Level 2 FORM (First Order Reliability Method) reliability analysis can be carried out. This study would require the development of a limit state equation in order to express the plastic moment capacity. With this equation, the statistical stochastic plastic moment capacity is expressed explicitly, and the dimensional tolerances can then be tested with a number of variations. With the results from these variations, the importance factor of each dimensional variable can be defined and compared to the ones presented in this study.

2. A database can be established and shared with university laboratories that test steel beams. To ensure accurate comparative analysis, 2000 samples of the same section size need to be collected. Of course, technicalities like the precision of measurement techniques and testing regimes need to be taken into account.

3. As was established in Chapter 4 of this dissertation, a convergence test was carried out for one beam (IPE360). This test (applied only for Test 1, where all the variables are randomised) deemed that 2000 samples was a sufficient number of samples since when compared to the result of the 20000 samples there was only a 3% margin of error. However, for further accuracy, similar convergence tests should be conducted for all beam sizes, especially since the tolerance ranges vary across different section sizes. In addition to this, further research could involve adjusting the intervals of these ranges to better understand the accuracy of the Monte Carlo

Simulation. During the current study, an in-depth analysis was conducted on 3 beams; in future this can be carried out for all sections in order to verify that all observations follow the patterns that have been identified throughout this study.

4. Another interesting study would involve considering these dimensional tolerances not as an individual structural element but as part of a structural system, such as a steel frame. The aim would be to provide a better understanding of the importance of first-order initial (dimensional) imperfections that can affect the load-bearing capacity of the structure.

References

Byfield, M. P., & Nethercot, D. A. (1997). Material and geometric properties of structural steel for use in design.

Byun, S. (2019). Managing tolerance stack-up through process integration team in steel industry. *Annals of Business Administrative Science, 18*(6), 223. 10.7880/abas.0191002a

Di Lorenzo, G., Formisano, A., & Landolfo, R. (2017). *On the Origin of I Beams and Quick Analysis on the Structural Efficiency of Hot-rolled Steel Members*. Bentham Science Publishers Ltd. 10.2174/1874149501711010332

European Committee for Standardization. (2005). *Eurocode 3: Design of steel structures – Part 1 -1: General rules and rules for buildings*

Popov, E. P. (1998). *Mechanics of Materials* (2nd Edition ed.). Pearson.

Hearn, E. J. (1997). *Mechanics of Materials Volume 1: An Introduction to the Mechanics of Elastic and Plastic Deformation of Solids and Structural Materials* (3rd Edition ed.). Butterworth-Heinemann.

Epri, D., & Gandy. (2006). *Carbon Steel Handbook*

Ferrous metals – plain carbon steels. https://engineersfield.com/ferrous-metals-plain-carbon-steels/

Gentle, J. E. (2003). *Random number generation and Monte Carlo methods* (2. ed. ed.). Springer.

Gavin, H. P. (2015). *Plastic Analysis of Beams*

Kala, Z. (2015). *Sensitivity and reliability analyses of lateral-torsional buckling resistance of steel beams*. Springer Science and Business Media LLC. 10.1016/j.acme.2015.03.007

Melcher, J., Kala, Z., Holický, M., Fajkus, M., & Rozlívka, L. (2020). *Design characteristics of structural steels based on statistical analysis of metallurgical products*. Elsevier BV. 10.1016/s0143-974x(03)00144-5

Melcher, R. E. (1987). *Structural reliability : analysis and prediction*. Chichester, W. Sussex, England : Ellis Horwood ; New York : Wiley.

Moynihan, M. C., & Allwood, J. M. (2024). *Utilization of structural steel in buildings*. The Royal Society. 10.1098/rspa.2014.0170

RStudio Team,(2020, *RStudio Team (2020). RStudio: Integrated Development for R. RStudio, PBC, Boston.* http://www.rstudio.com/.

Rubinstein, R. Y., & Kroese, D. P. (2008). *Simulation and the Monte Carlo method, second edition* (2nd ed. ed.). Wiley. 10.1002/9780470230381

Swift, K. G., Raines, M., & Booker, J. D. (2010). *Case studies in probabilistic design*. Informa UK Limited. 10.1080/09544820010000926

Yu, T. X., & Zhang, L.C. (1996). *Series on Engineering Mechanics: Volume 2 Plastic Bending: Theory and Applications*https://doi.org/10.1142/2754

Thoft-Christensen, P., Baker, M.J. (1982). *Fundamentals of Structural Reliability Theory. In: Structural Reliability Theory and Its Applications*. Springer, Berlin, Heidelberg. https://doi.org/10.1007/978-3-642-68697-9_4

Philpot, T, A., (2019). *Mechanics of Materials: An Integrated Learning System, 5th Edition*. Wiley.

Johnson, W & Mellor P,B. (1962). *Plasticity for mechanical engineers* (First Edition ed.). D. Van Nostrand Co., Inc;.

Weinzierl, S. (2000). *Introduction to Monte Carlo methods*

Williams, E. (1956). *Hooke's law and the concept of the elastic limit*. Informa UK Limited.

10.1080/00033795600200056

Appendix A

A.1 Microsoft Excel - VBA Code

To randomly generate 2000 numbers from a given range, the code below was used in VBA;

```
Sub GenerateRandomNumbers()
    Dim rngList As Range
    Dim randomIndex As Integer
    Dim numRows As Integer
    Dim i As Integer
    ' Set the range where your list of numbers is located
    Set rngList = ThisWorkbook.Sheets("600").Range("A27:A187")
    ' Specify the number of random numbers to generate
    numRows = 2000 ' Number of cells in column B where you want to place random numbers
    ' Clear previous results in column B
    ThisWorkbook.Sheets("600").Range("B457:B2457").Clear
    ' Generate random numbers and place them in column B
    For i = 1 To numRows
        ' Generate a random index
        randomIndex = Application.WorksheetFunction.RandBetween(1, rngList.Rows.Count)
        ' Get the randomly selected number and place it in column B
        ThisWorkbook.Sheets("600").Cells(i + 457, 2).Value = rngList.Cells(randomIndex, 1).Value
    Next i
End Sub
```

Appendix B

B.1 RStudio Code | For Test 1

```
1   #test 1- all variables. green=pass, red=fail

2   ggplot(TEST1, aes(x=TEST1$`WIDTH OF SECTION`, y=TEST1$`FLANGE THICKNESS`,
    fill=TEST1$`WEB THICKNESS`, color=factor(TEST1$`No. of failure`))) +
    geom_point(shape=21) +
3   scale_fill_continuous(name="Web Thickness")+
4   scale_colour_manual(name = "Result", labels = c("Pass", "Failure"),values =
    c("chartreuse", "red")) +
5   labs(y= "Flange Thickness", x = "Width of Section") +
6   theme_bw()+
7   scale_x_continuous(breaks = seq(min(TEST1$`WIDTH OF SECTION`), max(TEST1$`WIDTH
    OF SECTION`),by=1))+
8   scale_y_continuous(breaks = seq(min(TEST1$`FLANGE THICKNESS`),
    max(TEST1$`FLANGE THICKNESS`),by=1))+
9   geom_vline(xintercept = 267)+
10  geom_hline(yintercept = 21.6)
```

B.2 RStudio Code | For Test 2

```
1   #test 2- yield stress fixed. green=pass, red=fail

2   ggplot(TEST2, aes(x=TEST2$`WIDTH OF SECTION`, y=TEST2$`FLANGE THICKNESS`,
    fill=TEST2$`WEB THICKNESS`, color=factor(TEST2$`No. of failure`))) +
    geom_point(shape=21) +
3   scale_fill_continuous(name="Web Thickness")+
4   scale_colour_manual(name = "Result", labels = c("Pass", "Failure"),values =
    c("chartreuse", "red")) +
5   labs(y= "Flange Thickness", x = "Width of Section") +
6   theme_bw()+
7   scale_x_continuous(breaks = seq(min(TEST2$`WIDTH OF SECTION`), max(TEST2$`WIDTH
    OF SECTION`),by=1))+
8   scale_y_continuous(breaks = seq(min(TEST2$`FLANGE THICKNESS`),
    max(TEST2$`FLANGE THICKNESS`),by=1))+
9   geom_vline(xintercept = 267)+
10  geom_hline(yintercept = 21.6)
```

B.3 RStudio Code | For Test 7 to Test 16

```
1   #test 3- yield stress and another variable fixed. green=pass, red=fail

2   ggplot(TEST7, aes(x=TEST7$`WIDTH OF SECTION`, y=TEST7$`FLANGE THICKNESS`, fill=TEST7$`WEB THICKNESS`, color=factor(TEST7$`No. of failure`))) + geom_point(shape=21) +
3   scale_fill_continuous(name="Web Thickness")+
4   scale_colour_manual(name = "Result", labels = c("Pass", "Failure"),values = c("chartreuse", "red")) +
5   labs(y= "Flange Thickness", x = "Width of Section") +
6   theme_bw()+
7   scale_x_continuous(breaks = seq(min(TEST7$`WIDTH OF SECTION`), max(TEST7$`WIDTH OF SECTION`),by=1))+
8   scale_y_continuous(breaks = seq(min(TEST7$`FLANGE THICKNESS`), max(TEST7$`FLANGE THICKNESS`),by=1))+
9   geom_vline(xintercept = 267)+
10  geom_hline(yintercept = 21.6)
```

B.4 RStudio Code | For Test 1 - Test 2

```
1   #difference between tests 1 and 2. shows the impact of yield stress alone.

2   diff_t1t2 <- -(TEST1$`No. of failure` - TEST2$`No. of failure`)
3   TEST2$diff <- diff_t1t2
4   fails<-TEST2[TEST2$diff !=0, ]
5   ggplot(fails, aes(x=fails$`WIDTH OF SECTION`, y=fails$`FLANGE THICKNESS`,
    fill=fails$`WEB THICKNESS`, color=factor(fails$`diff`))) + geom_point(shape=21) +
6   scale_fill_continuous(name="Web Thickness")+
7   scale_colour_manual(name = "Result", labels = c("Fail T1, Pass T2", "Pass T1, Fail
    T2"),values = c("deeppink", "black")) +
8   labs(y= "Flange Thickness", x = "Width of Section") + theme_bw()+
9   scale_x_continuous(breaks = seq(min(fails$`WIDTH OF SECTION`), max(fails$`WIDTH OF
    SECTION`),by=1))+
10  scale_y_continuous(breaks = seq(min(fails$`FLANGE THICKNESS`), max(fails$`FLANGE
    THICKNESS`),by=1))+
11  geom_vline(xintercept = 267)+
12  geom_hline(yintercept = 21.6)
```

B.5 Rstudio Code | For Test 2 – Test 7/8/9/10

```
#difference between tests 2 and 3. shows the impact of the other fixed variable

diff_t2t3 <- -(TEST2$`No. of failure` - TEST7$`No. of failure`)
TEST7$diff_t2 <- diff_t2t3
fails3<-TEST7[TEST7$diff_t2 !=0, ]
ggplot(fails3, aes(x=fails3$`WIDTH OF SECTION`, y=fails3$`FLANGE THICKNESS`, fill=fails3$`WEB THICKNESS`, color=factor(fails3$`diff_t2`))) + geom_point(shape=21) +
scale_fill_continuous(name="Web Thickness")+
scale_colour_manual(name = "Result", labels = c("Fail T2, Pass T3", "Pass T2, Fail T3"),values = c("deeppink", "black")) +
labs(y= "Flange Thickness", x = "Width of Section") + theme_bw()+
scale_x_continuous(breaks = seq(min(fails3$`WIDTH OF SECTION`), max(fails3$`WIDTH OF SECTION`),by=1))+
scale_y_continuous(breaks = seq(min(fails3$`FLANGE THICKNESS`), max(fails3$`FLANGE THICKNESS`),by=1))+
geom_vline(xintercept = 267)+
geom_hline(yintercept = 21.6)
```

Appendix C

C.1 Further Results | Test 11 to Test 16

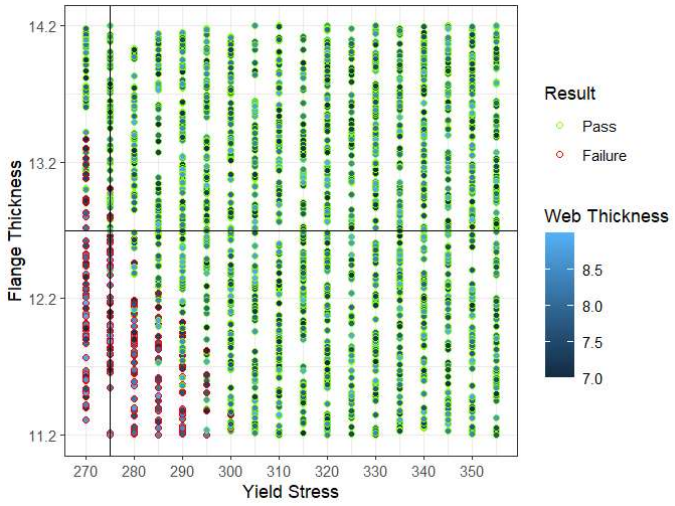

Figure C.1 Test 11 | IPE360

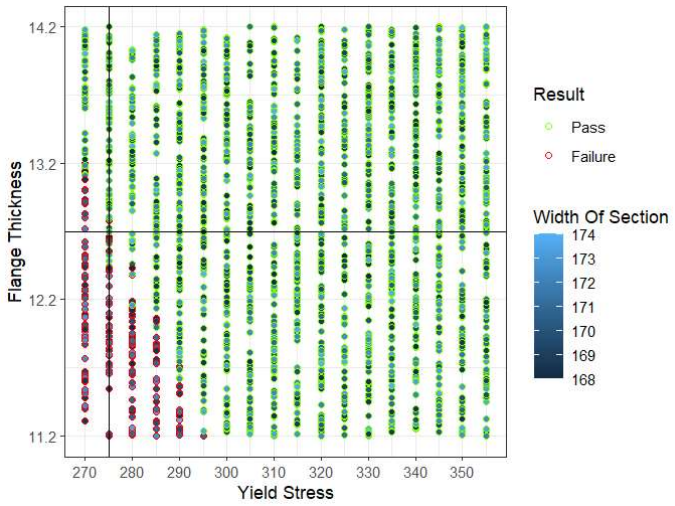

Figure C.2 Test 12 | IPE360

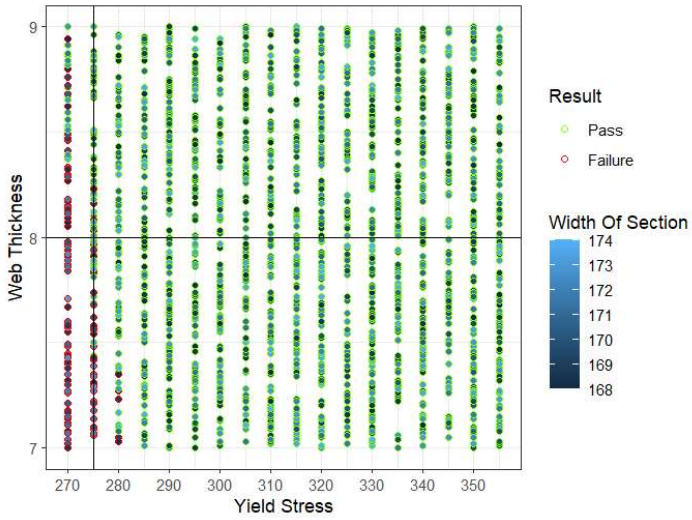

Figure C.3 Test 13 | IPE360

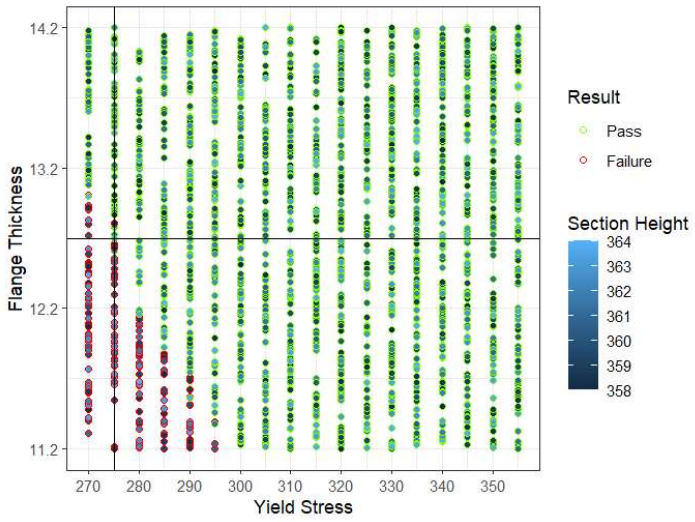

Figure C.4 Test 14 | IPE360

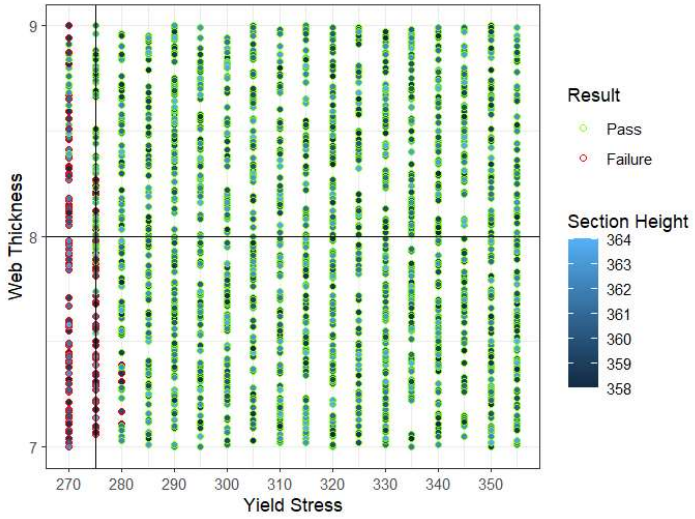

Figure C.5 Test 15 | IPE360

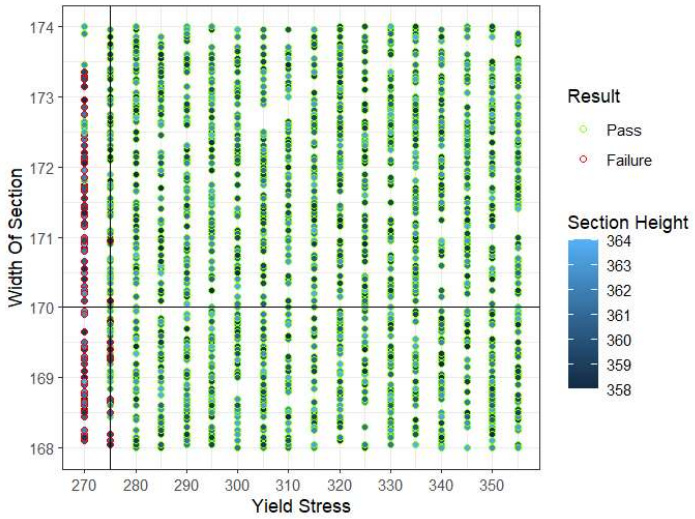

Figure C.6 Test 16 | IPE360

C.2 Further Results | Test 2 – Test 7

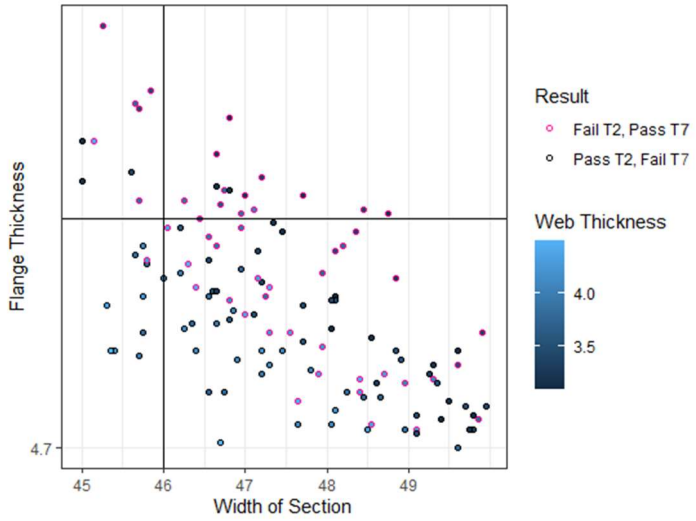

Figure C.7 Test 2 – Test 7 | IPE80

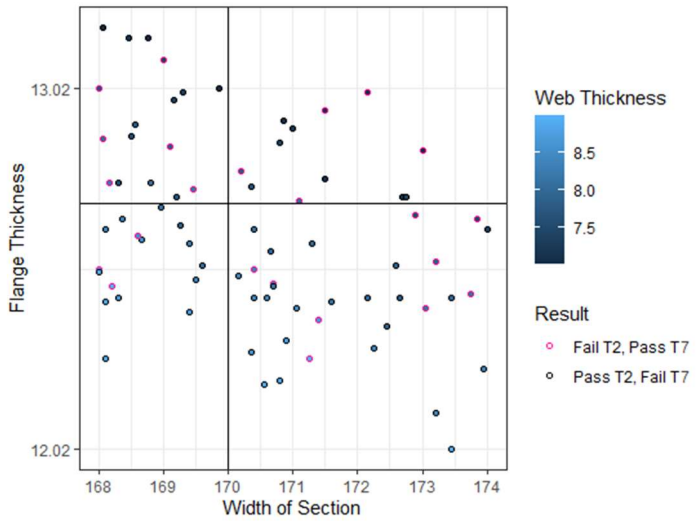

Figure C.8 Test 2 – Test 7 | IPE360

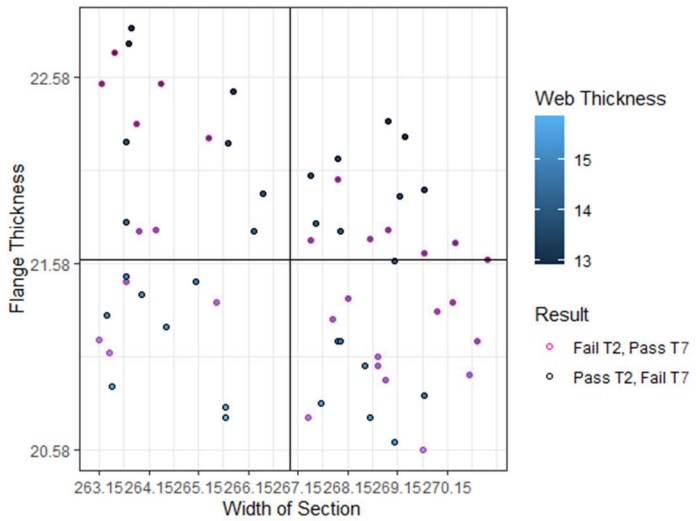

Figure C.9 Test 2 – Test 7 | IPE750x173

C.3 Further Results | Test 2 – Test 8

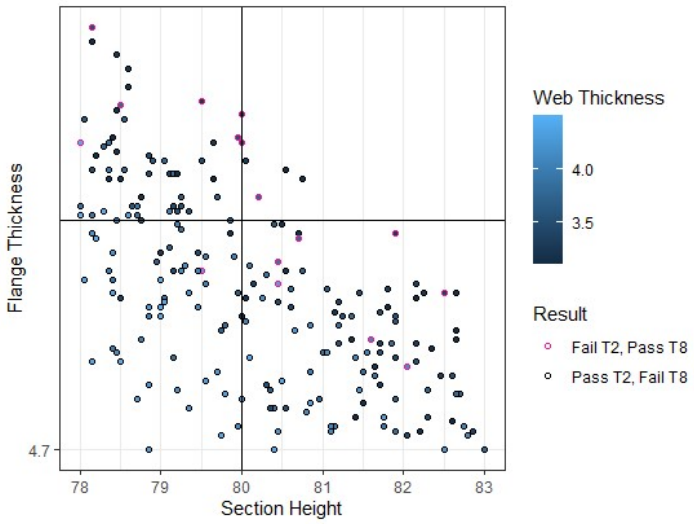

Figure C.10 Test 2 – Test 8 | IPE80

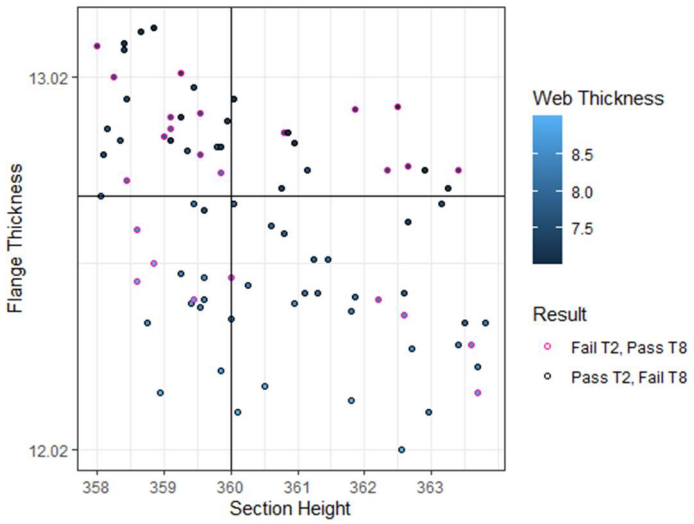

Figure C.11 Test 2 – Test 8 | IPE360

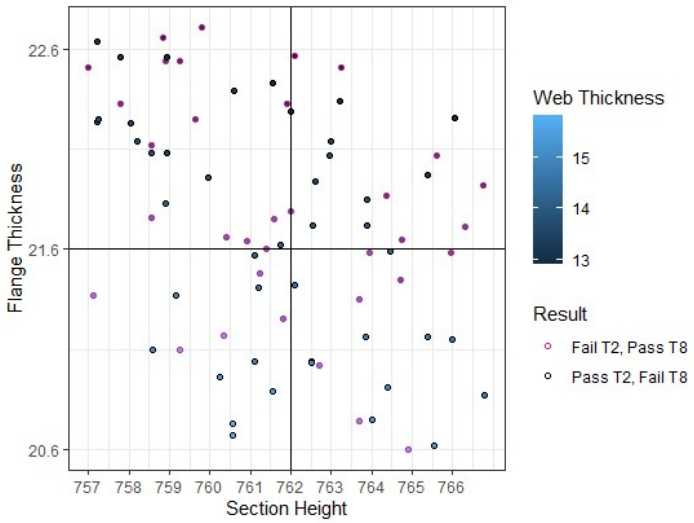

Figure C.12 Test 2 – Test 8 | IPE750x173

C.4 Further Results | Test 2 – Test 9

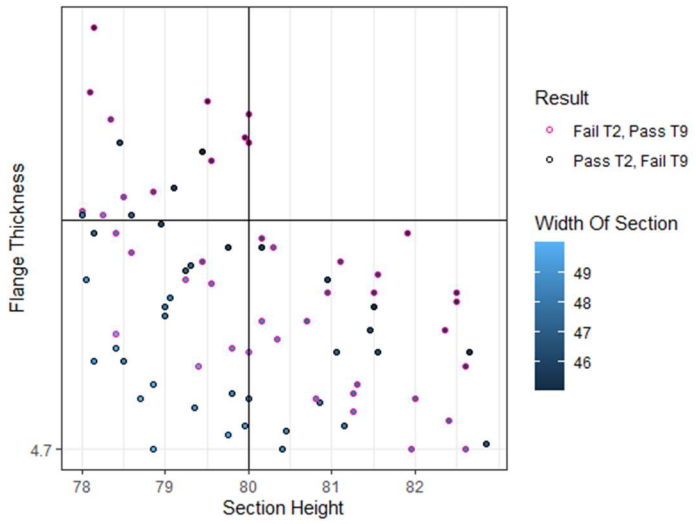

Figure C.13 Test 2 – Test 9 | IPE80

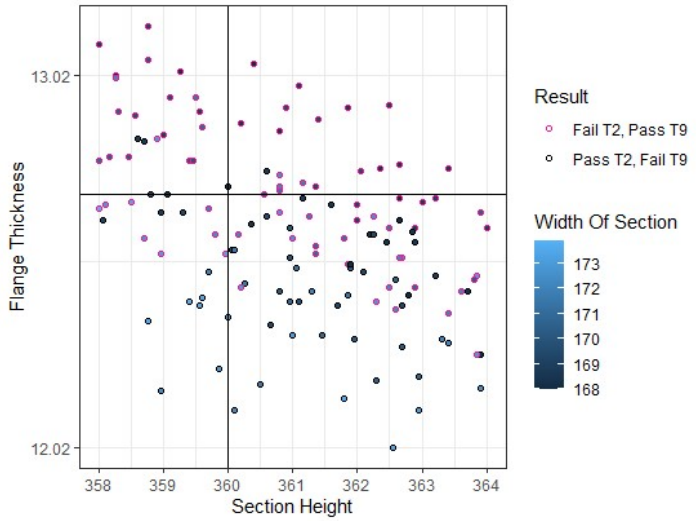

Figure C.14 Test 2 – Test 9 | IPE360

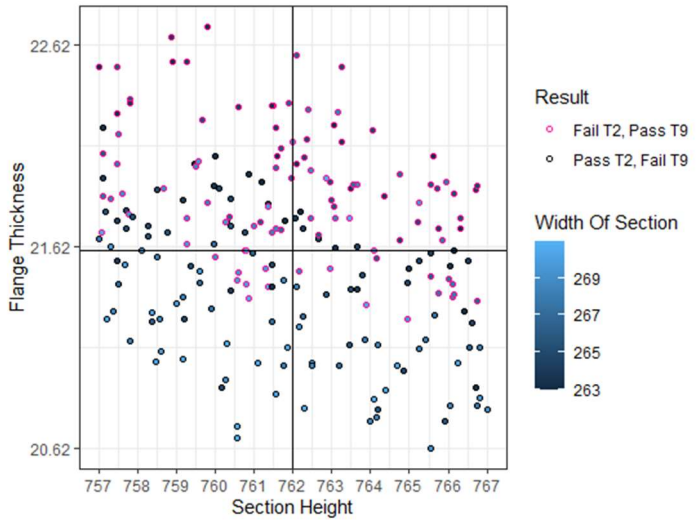

Figure C.15 Test 2 – Test 9 | IPE750x173

C.5 Further Results | Test 2 – Test 10

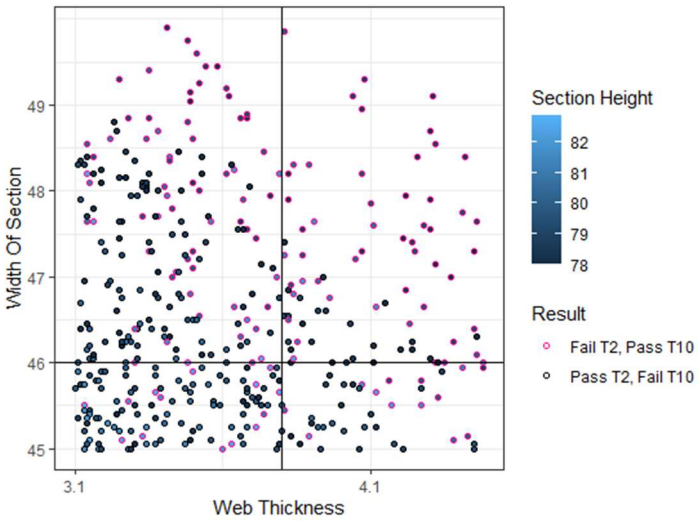

Figure C.16 Test 2 – Test 10 | IPE80

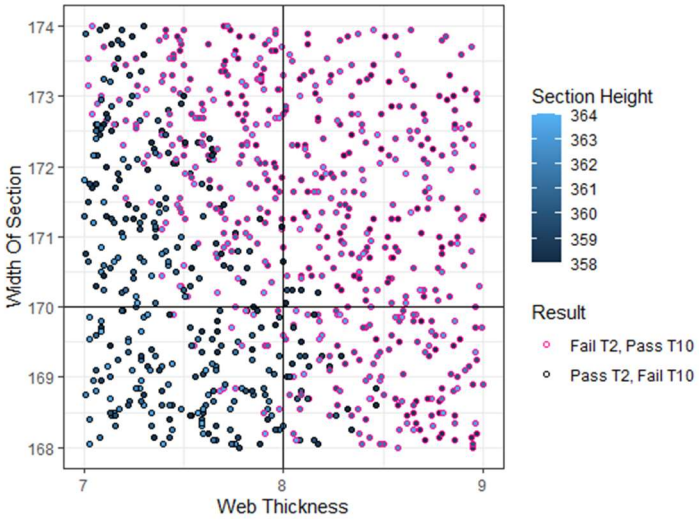

Figure C.17 Test 2 – Test 10 | IPE360

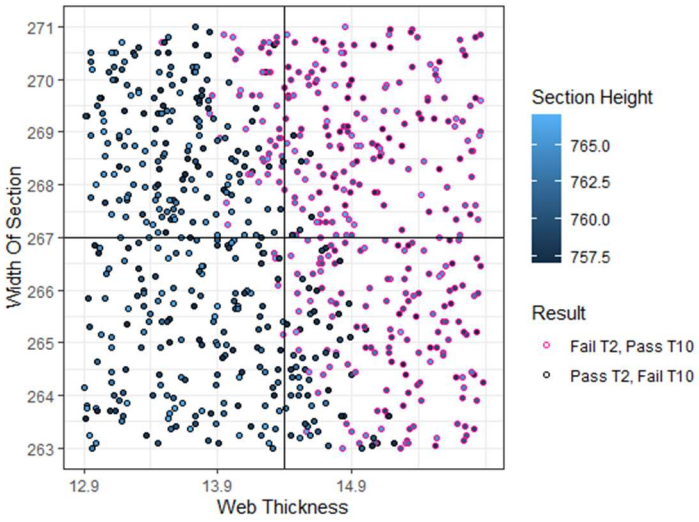

Figure C.18 Test 2 – Test 10 | IPE750x173

C.6 Further Results |

Each beam was assigned a distinct colour to facilitate a clearer analysis of potential correlations. The study involved comparing the rankings of upper and lower bound tolerances—divided by the nominal value—with the rankings of the probability of failure to identify any correlation and to explore the reasons why tolerances do not relate proportionally to the section size. Another analysis involved calculating the difference between the combined tolerances divided by the nominal value. This process was carried out on Microsoft Excel, where each colour represents a specific beam, and the columns display rankings from smallest to largest (as graphically presented in the figures below).

From this analysis, it can be concluded that the tolerances did not reveal any significant correlations between these ratios and the probability of failure, suggesting that no discernible trends are indicating that the range of tolerances correlates directly with section depth. However, it is noteworthy that there is a strong correlation across all beam sizes between the ranking of the upper bound tolerances for all four geometric dimensions and the ranking of the range of tolerances (upper bound - lower bound) for these dimensions. Despite this finding, these correlations do not significantly impact the broader context of the study.

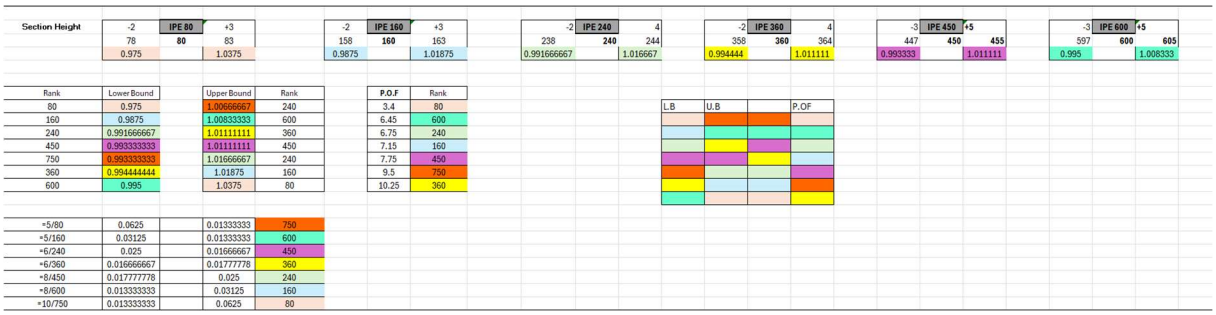

Figure C.19 The ranking of the lower bound, upper bound and range of tolerances vs the ranking of the Probability of Failure for Section Height tolerances

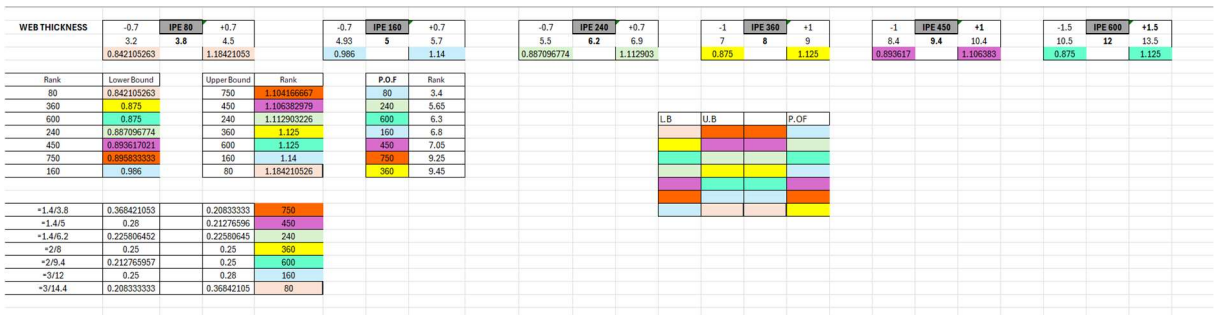

Figure C.20 The ranking of the lower bound, upper bound and range of tolerances vs the ranking of the Probability of Failure for Width of Section Tolerances

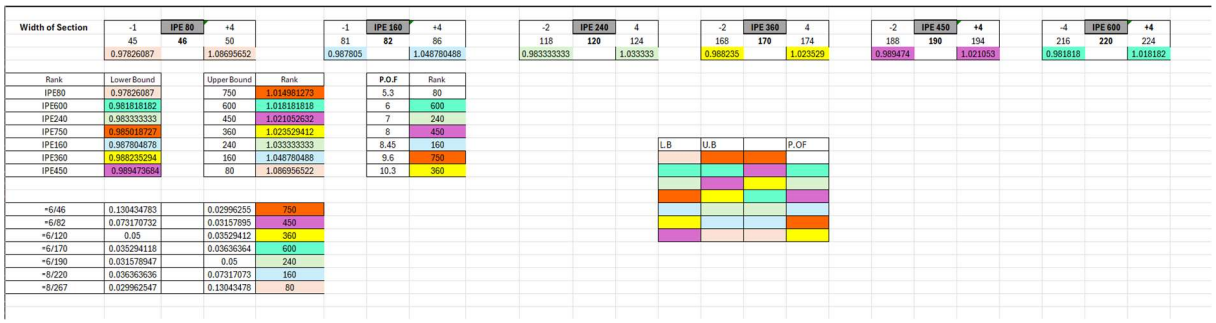

Width of Section	-1	IPE 80	+4	-1	IPE 160	+4	-2	IPE 240	4	-2	IPE 360	4	-2	IPE 450	+4	-4	IPE 600	+4
	45	46	50	81	82	86	118	120	124	168	170	174	188	190	194	216	220	224
	0.97826087		1.08695652	0.987805		1.048780488	0.983333333		1.033333	0.988235		1.023529	0.989474		1.021053	0.981818		1.018182

Rank	Lower Bound	Upper Bound	Rank	P.O.F	Rank
IPE80	0.97826087	750	1.014981273	5.3	80
IPE600	0.981818182	600	1.018181818	6	600
IPE240	0.983333333	450	1.021052632	7	240
IPE750	0.985018727	360	1.023529412	8	450
IPE160	0.987804878	240	1.033333333	8.45	160
IPE360	0.988235294	160	1.048780488	9.6	750
IPE450	0.989473684	80	1.086956522	10.3	360

÷6/46	0.130434783	0.02996255	750
÷6/82	0.073170732	0.03157895	450
÷6/120	0.05	0.03529412	360
÷6/170	0.035294118	0.03636364	600
÷6/190	0.031578947	0.05	240
÷8/220	0.036363636	0.07317073	160
÷8/267	0.029962547	0.13043478	80

L.B	U.B		P.OF

Figure C.13 The ranking of the lower bound, upper bound and range of tolerances vs the ranking of the Probability of Failure for Web Thickness Tolerances

FLANGE THICKNESS	-0.5	IPE 80	+1.5	-1	IPE 160	+2	-1.5	IPE 240	+2.5	-1.5	IPE 360	+2.5	-1.5	IPE 450	+2.5	-1.5	IPE 600	+2.5
	4.7	5.2	6.7	6.4	7.4	9.4	8.3	9.8	12.3	11.2	12.7	15.2	13.1	14.6	17.1	17.5	19	21.5
	0.903846154		1.28846154	0.864865		1.27027027	0.846938776		1.255102	0.88189		1.19685	0.89726		1.171233	0.921053		1.131579

Rank	Lower Bound	Upper Bound	Rank	P.O.F	Rank
	0.846938776		1.115740741	80	3.6
	0.864864865		1.131578947	160	4.15
	0.881889764		1.171232877	240	5.4
	0.897260274		1.196650394	360	5.8
	0.903846154		1.255102041	600	6.9
	0.907407407		1.27027027	450	7.05
	0.921052632		1.288461538	750	8.15

÷2/5.2	0.384615385			
÷4.5/21.6	0.208333333			
÷4/4/19	0.210526316			
÷4/14.6	0.273972603			
÷4/12.7	0.31496063			
÷3/7.4	0.405405405			
÷4/9.8	0.408163265			

L.B	U.B		P.OF

Figure C.22 Figure C.14 The ranking of the lower bound, upper bound and range of tolerances vs the ranking of the Probability of Failure for Flange Thickness Tolerances